Zeotropic mixtures R1234ze(Z)/acetone and R1234ze(Z)/isohexane as refrigerants in high temperature heat pumps: Influence of the accuracy in thermodynamic properties evaluations

Zeotropic Mixtures R1234ze(Z)/acetone and R1234ze(Z)/isohexane as Refrigerants in High Temperature Heat Pumps: influence of the accuracy in thermodynamic properties evaluations

Hamed Abedini[a], Sebastiano Tomassetti[b], Giovanni Di Nicola[b], Sylvain Quoilin[a], Alessia Arteconi[a,b,c,*]

[a] *Mechanical Engineering Department, KU Leuven, Leuven 3000, Belgium*

[b]*Dipartimento di Ingegneria Industriale e Scienze Matematiche, Università Politecnica delle Marche, 60131, Ancona, Italy*

[c]*EnergyVille, 3600, Genk, Belgium*

** Corresponding author. Email address: alessia.arteconi@kuleuven.be, Tel.: +32 14 72 14 68*

Abstract

High temperature heat pumps (HTHPs) represent an interesting option to upgrade waste heat up to 200°C for industrial application. In order to achieve such high temperatures, suitable refrigerants are needed. In this paper, two zeotropic mixtures composed of a hydrofluoro-olefin (HFO) and a hydrocarbon, namely R1234ze(Z)/acetone and R1234ze(Z)/isohexane, were examined as the refrigerant for HTHP applications. The main objective of the present study is to determine the binary interaction parameters (BIPs) of the two zeotropic mixtures from experimentally-determined thermodynamic properties and analyse how HTHP performance assessment would change after tuning the BIPs. For R1234ze(Z)/acetone, after tuning the BIPs, the phase change temperature glide did not change that much. However, the composition corresponding to the highest temperature glide changed significantly. On the other hand, for R1234ze(Z)/isohexane, the phase change temperature glide changed significantly with tuned BIPs, while the composition for the maximum temperature glide was quite similar in the two cases. A thermodynamic optimization framework was used for simulation of the HTHP cycle. Simulation results using estimated BIPs showed that for R1234ze(Z)/acetone the optimum coefficient of performance (COP) was 3.95, while it slightly changed to 3.94 (around 0.25% change) after tuning the BIPs. However, the optimum composition of the mixture was quite different for the estimated and fitted BIPs. For R1234ze(Z)/isohexane the COP was 3.90 using estimated BIPs, while it changed to 3.83 (around 1.7% change) once the fitted BIPs were used. These results indicate the importance of tuning the BIPs for zeotropic mixtures and different impacts depending on the performance parameters analysed.

Keywords: zeotropic mixture; binary interaction parameters; heat pump; thermodynamics model; temperature glide

Nomenclature

Symbols:

p	*pressure*	*[bar]*
z_1	*overall mole fraction*	
y_1	*mole fraction in vapor phase*	
x_1	*mole fraction in liquid phase*	
T	*temperature*	*[°C]*
v	*specific volume*	*[m^3/kg]*
β, γ	*binary interaction parameters*	

Subscripts

b	*boiling point*
c	*critical*
calc	*calculated*
cd	*condenser*
ev	*evaporator*
exp	*experimental*
in	*inlet*
is	*isentropic*
out	*outlet*
sc	*subcooling*
sh	*superheat*
si	*sink*
so	*source*

Abbreviations:

AARD	*average absolute relative deviations*
BIP	*binary interaction parameter*
COP	*coefficient of performance*
GWP	*global warming potential*
HC	*hydrocarbon*
HCFO	*hydrochlorofluoro-olefin*
HFC	*hydrofluorocarbon*
HFO	*hydrofluoro-olefin*
HTHP	*high temperature heat pump*
IHX	*internal heat exchanger*
ODP	*ozone depletion potential*
PPTD	*pinch point temperature difference*
TXV	*thermal expansion valve*
VHTHP	*very high temperature heat pump*

1. Introduction

Industry is the largest heat-consuming final sector accounting for nearly 46% of the world total energy use for heating [1]. Beside space heating and hot water, there is a great demand for process heating in industry for the production, the processing, or the finishing of products. Generally, process heating is supplied above 80°C and below that threshold is considered waste heat [2]. The potential for upgrading waste industrial heat into useful thermal energy in the temperature range between 100 and 200°C to be used again in the processes is huge. Indeed, the waste heat potential in Europe is estimated around 300 TWh/y and about 20% of thermal energy demand has a temperature between 100-200°C [3]. Waste heat recovery is recommended to increase energy efficiency and reduce CO_2 emissions of energy intensive industrial sectors (e.g. chemical industry). However, the thermal demand and the operating temperatures depend strictly on the considered industrial process and on the specific working conditions, thus adaptable solutions are crucial.

High temperature heat pumps (HTHPs), defined typically as having a sink temperature (i.e. the temperature of the useful heat being produced) above 100°C, find an interesting application potential in such heat recovery in industrial processes [4]. According to the IEA Roadmap [5], the electrification of the thermal demand will play an important role (around 40% of heat demand by 2030 and about 65% by 2050) with heat pumps accounting for about 30% of the total heat demand below 400 °C in 2050. The current state-of-the-art of HTHPs remains limited in terms of heat sink temperature achievable. According to Arpagaus et al. [2] HTHPs with heat sink from 80°C to 100°C are commercially available. However, from 100°C to 140°C, they are in the development phase, and above 140°C, they are still at the stage of laboratory research. For HTHPs the most relevant working fluid properties to take into considerations are [6]: high thermodynamic critical point (for sub-critical cycles); chemical stability in the full operating temperature range; small specific volume value of the saturated vapour prior to the compressor (to reduce compressor size); high value of heat transfer coefficient in evaporation and condensation processes (to reduce heat exchangers size); low viscosity (to reduce pressure drops); good environmental (local and global) properties (ozone depletion potential (ODP) equal to 0, global warming potential (GWP) lower than 150, limited flammability and toxicity); low cost.

At present the most used refrigerants in commercial HTHPs are R245fa, R717, R744, R134a, and R1234ze(E) [2]. More generally, a number of commercially available working fluids on the market were identified to reach theoretically a maximum temperature of 165 °C [2]: R365mfc, R245ca, R245fa that are hydrofluorocarbons (HFCs); R1336mzz(Z), R1234ze(Z) that are hydrofluoro-olefin (HFOs); R1233zd (E), R1224yd(Z) that are hydrochlorofluoro-olefins (HCFOs); R601, R600 that are hydrocarbons (HCs); Novec649 that is a fluorinated ketone; R718, R717 that are natural refrigerants.

HFCs are already commonly used in other applications, as organic Rankine cycles (ORCs). However, their GWP is usually high (>150), which is detrimental to climate targets and will lead to their phasing out in Europe through the F-gas regulation [7]. HFOs are a promising, new generation of working fluids which recently appeared on the market, but there are some concerns about their chemical stability and mild flammability (e.g. R1234ze(E) and R1234ze(Z) are classified A2L). HCs such as butane or pentane are already widely used in refrigeration and ORC systems. Their low cost is particularly appealing but a critical issue regards their flammability (A3). Among the most promising working fluids there are R1234ze(Z), R1233zd(E) and R1336mzz(Z), which have been used in ORCs at higher temperatures [8]. Although in an early stage for use in industrial HTHPs [2], their thermodynamic properties are well known and theoretical

studies have discussed their potential benefits in terms of reduced compressor size and coefficient of performance (COP) increase [9]. These fluids present excellent properties in terms of ODP (≈0), GWP (<5), flammability and toxicity (A1 and A2L) and chemical stability (demonstrated up to 250°C). They only appeared commercially in the last years and their accurate equations of states have only been fitted recently [2]. The availability of these new fluids opens a broad range of possibilities for HTHPs and highlights the need for further R&D in that field. Indeed their critical temperatures are 171.3°C for R1336mzz(Z) and 150.1°C for R1234ze(Z), which is below the target temperature of 200°C aimed in this paper. For this reason, it is valuable to explore the possibility of mixing them with other fluids which can increase the fluid critical temperature. Indeed, by adjusting the composition of a blend, it is possible to modify the critical point, the pressure levels and the vapour densities to match them to the target process. In particular it has been demonstrated [10] that zeotropic mixtures can help matching the sink/load temperature variation due to their temperature glide, resulting in this way suitable for several industrial applications.

In this paper a zeotropic mixture of a HFO and a hydrocarbon is considered as a refrigerant for HTHPs delivering heat up to 200°C. The former for its good environmental properties and the latter for the high critical temperature. With more detail, R1234ze(Z)/acetone and R1234ze(Z)/isohexane have been selected for the good properties as refrigerants obtained from a preliminary assessment [11]. These mixtures were not used before in this kind of applications and the thermodynamic properties of the mixtures are not fully known. This paper aims at shading a light on new possible zeotropic mixtures to be used in high temperature heat pumps applications by improving the knowledge on the thermodynamic properties of unknown mixtures. In particular, purpose of this paper is (i) to perform experimental measurements to define the real behaviour of the considered mixtures and (ii) to assess their performance in a reverse vapour compression cycle of a HTHP. Eventually the impact of the accuracy of such thermodynamic properties of the mixture is discussed and general conclusions are drawn on the applicability of the proposed mixtures.

2. Methodology

In this paper, two zeotropic mixtures composed of a hydrofluoro-olefin (HFO) and a hydrocarbon, namely R1234ze(Z)/acetone and R1234ze(Z)/isohexane, have been considered as refrigerant for HTHP applications. Given that for these two mixtures the binary interaction parameters (BIPs) are not available and the database REFPROP 10.0 uses estimated values, various two-phase and vapor phase *pvTz* measurements were performed. The BIPs were tuned by minimizing the difference between the measured pressures and estimated pressures. The fitted and estimated values of the BIPs were then used in a thermodynamic model to assess the performance of the HTHP cycle with these mixtures and the impact of the error that could be made without an accurate knowledge of the properties of the refrigerants.

2.1. Selected zeotropic mixtures

In our previous work [11], various binary mixtures available in REFPROP 10.0 were thermodynamically tested as refrigerant in VHTHPs. It was shown that binary mixtures composed of an hydrofluoro-olefin (HFO) and a hydrocarbon could be a good option due to their phase change temperature glide which can be matched with the temperature profile of the sink and the source. Based on our previous analysis, R1234ze(Z)/acetone and R1234ze(Z)/isohexane are two examples of such mixtures that resulted in high COPs, high volumetric heating capacity (VHC) and reasonable compressor exhaust temperature [11].

These mixtures were selected in this study for further analysis. The main physical properties of the constituent pure fluids (R1234ze(Z), acetone and isohexane) are reported in Table 1.

Table 1. Main physical properties of R1234ze(Z), acetone and isohexane.

Compound	T_c (°C)[12]	P_c (bar) [12]	T_b (°C) [12]	GWP	ODP
R1234ze(Z)	150.1	35.3	9.7	<1[13]	0[13]
acetone	235.0	46.9	56.1	1.6[14]	10^{-7} [14]
isohexane	224.6	30.4	60.2	< 6[9]	0[9]

2.2. Isochoric apparatus

In this section the experimental procedure is described. The samples of the fluids used, *cis*-1,3,3,3-tetrafluoroprop-1-ene (R1234ze(Z), CAS number 29118-25-0), acetone (CAS number 67-64-1), and isohexane (CAS number 107-83-5) were supplied by Central Glass Ltd., Honeywell, and Thermo Fisher Scientific, respectively. The purities of the samples declared by the suppliers were as follows: >99% for R1234ze(Z), >99.5% for acetone, and >99% for isohexane.

2.2.1. Experimental setup and procedure

Considering that the experimental setup, test procedure, and experimental uncertainties were described in previous studies [15-18], only a summary is provided below. As shown in Figure 1, the isochoric setup comprised a constant-volume AISI 304 stainless steel sphere with a volume of approximatively 273.5 cm^3 at 35 °C and two thermostatic baths covering the temperature range from (-60 to 120) °C. The pressure was measured by using a Ruska 7000 pressure transducer coupled to an electronic null indicator. The temperature set-point was maintained through a PID device coupled with a 25 Ω platinum resistance thermometer (Hart Scientific 5680). From the propagation of uncertainty, the expanded uncertainties in temperatures, pressures, and volumes at the 95 % confidence level were determined to be 0.03 °C, 0.01 bar, 0.3 cm^3, respectively.

The gravimetric method was used to charge the samples in the experimental setup. As first step, after evacuating the measuring cell, tubing and connections with a vacuum pump, the desired mass of low-pressure liquid sample (acetone or isohexane) contained in a glass syringe was directly discharged into the isochoric sphere. The syringe was weighted with an analytical balance (uncertainty of ±0.3 mg) before and after the sample was discharged in the setup. The difference between the initial and final masses of the syringe allowed to determine the mass of liquid sample discharged in the experimental setup. The accuracy of this charging procedure for the liquid sample was checked by measuring 28 vapor-phase *pvT* data for acetone and 23 vapor-phase *pvT* data for isohexane. The measurements for acetone were carried out in the specific volume range from (0.138771 to 0.608462) $m^3 \cdot kg^{-1}$ and temperature range from (70 to 115) °C, while that for isohexane in the specific volume range from (0.095607 to 0.438115) $m^3 \cdot kg^{-1}$ and temperature range from (70 to 118) °C. The reliability of the charging procedure was verified by comparing the experimental pressures with that calculated from REFPROP 10.0 [12], obtaining average absolute relative deviations for the pressure (AARD(*p*)) equal to 0.24 % for acetone and 0.54 % for isohexane. In the measured temperature ranges, the Helmholtz-energy equations of state of the two fluids used in

REFPROP 10.0 have the following uncertainties in vapor pressure: 0.25 % for acetone and 0.2 % for isohexane. The AARD(p) has the following expression:

$$\mathrm{AARD}(p)/\% = \frac{100}{N}\sum_{i=1}^{N}\left|\frac{p_{\mathrm{exp,i}} - p_{\mathrm{calc,i}}}{p_{\mathrm{exp,i}}}\right| \quad (1)$$

where p_{exp} is the experimental pressure, p_{calc} is the calculated pressure and N is the number of experimental points. Then, the higher-pressure gas sample was charged by following the procedure presented in previous studies [17-19]. As described elsewhere [17-19], the uncertainties of masses, specific volumes, and mole fractions were estimated from the propagation of uncertainty. The expanded uncertainty in mass at the 95 % confidence level was determined to be 1.2 mg. The expanded uncertainties in specific volumes at the 95% confidence level for R1234ze(Z)/acetone and R1234ze(Z)/isohexane binary systems ranged from (0.109 to 0.337) $dm^3 \cdot kg^{-1}$ and from (0.081 to 0.332) $dm^3 \cdot kg^{-1}$, respectively. Instead, the expanded uncertainties in mole fractions at the 95% confidence level ranged from (0.001 to 0.003) for R1234ze(Z)/acetone and from (0.001 to 0.002) for R1234ze(Z)/isohexane.

After the samples were charged in the experimental setup, the measurements were carried out as follows: once the temperature of the thermostatic bath was stable at the temperature set-point, a circulating pump was turned on for about 20 minutes; the sample charged in the measuring cell was allowed to stabilize for about an hour; the pressure values were recorded. After that the temperature of the thermostatic bath was set to a different value, this procedure was repeated.

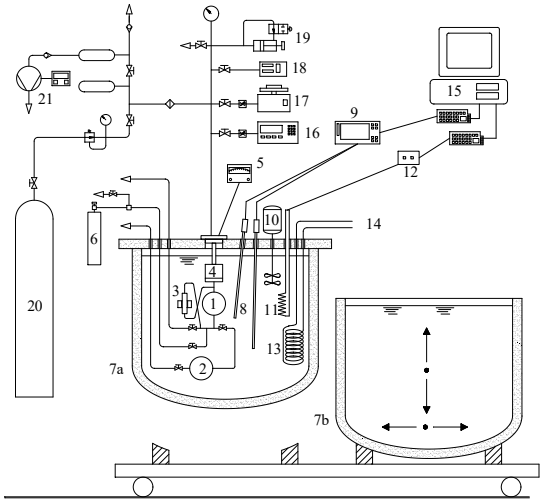

1	Constant volume spherical cell	12	Power system
2	Auxiliary cell	13	Cooling coil
3	Magnetic pump	14	Connections to auxiliary thermostatic bath
4	Differential pressure transducer	15	Acquisition system
5	Electronic null indicator	16	Bourdon gage
6	Charging system	17	Dead weight gage
7	Thermostatic baths	18	Vibrating cylinder pressure gage
8	Platinum thermo-resistances	19	Precision pressure controller
9	Thermometric bridge	20	Nitrogen reservoir

10 Stirrer
11 Heater
21 Vacuum pump system

Figure 1. Schematic view of the experimental isochoric setup.

2.3. Thermodynamic calculations

Properly tuned multi-fluid Helmholtz-energy explicit models can provide the most accurate descriptions of various thermodynamic properties of mixtures containing refrigerants [7]. These multi-fluid models are used in REFPROP 10.0 [12] to represent the thermodynamic properties of several mixtures. In the software, the models combine accurate equations of state implemented for the pure fluids with reducing functions and (optional) departure functions, that can be either specific to a particular binary system or generalized functions for a class of mixtures. Details about the models used in REFPROP 10.0 can be found in various literature studies [20, 21]. The multi-fluid Helmholtz-energy explicit models contains four adjustable binary interaction parameters (BIPs) for each *ij* binary pair ($\beta_{T,ij}$, $\beta_{v,ij}$, $\gamma_{T,ij}$, $\gamma_{v,ij}$) and a binary-specific multiplier (F_{ij}) for the departure function (when present). The BIPs used in REFPROP 10.0 for numerous binary pairs have been regressed on experimental thermophysical property data available in the literature. However, when no measurements are available for a binary system, the BIPs are estimated by following two possible methods [20]. This is the case for the selected binary mixtures (R1234ze(Z)/acetone and R1234ze(Z)/isohexane) in this study.

In order to have more accurate cycle simulations for these mixtures, their BIPs were identified from the assessment of the vapor-liquid equilibrium (VLE) by following the procedure described elsewhere [12, 22]. The VLE properties for R1234ze(Z)/acetone and R1234ze(Z)/isohexane binary systems were derived from the two-phase measurements, as described in the previous section, by employing the "flash method" with the multi-fluid Helmholtz-energy explicit model. These calculations were carried out by using both the estimated BIPs of the multi-fluid Helmholtz-energy explicit models available in REFPROP 10.0 [12] and the BIPs tuned on the presented experimental data measured in the two-phase region. The BIPs were tuned by minimizing the difference between the experimental two-phase pressures and the values calculated with the "flash method". The tuning of the BIPs was performed through the evolution strategy optimization algorithm [23] and by minimizing the following objective function:

$$Q = \sum_{i=1}^{N} \left(\frac{p_{\text{exp,i}} - p_{\text{calc,i}}}{p_{\text{exp,i}}} \right)^2 \tag{2}$$

Since a limited number of two-phase data were used in the BIP tuning, the parameters $\beta_{v,ij}$ and $\gamma_{v,ij}$ were set equal to 1 and no departure functions were adjusted. The abovementioned optimization algorithm was chosen because the evolutionary, or genetic, optimization routines were found to be robust and suitable solutions for the complexity of the fitting problem [24].

2.4. Simulation and optimization of the heat pump cycle

A reverse vapor compression heat pump cycle, as shown in Figure 1, was used for the evaluation of the selected mixtures as refrigerant in HTHP. The main components of this HTHP cycle are: the evaporator, condenser, the internal heat exchanger (IHX), the compressor and the thermal expansion valve (TXV). The thermodynamic model developed in our previous work [11] was used here for simulation of the HTHP cycle and optimization of the main cycle properties. In brief, it was assumed that the system operates under steady-state conditions. Heat loss and pressure drops in the system components and piping were neglected. The expansion in the TXV was isenthalpic and compressor operated with a fixed isentropic

efficiency of 0.75. REFPROP 10.0 (with estimated and fitted BIPs) was used for calculating the physical properties of the refrigerant mixtures. The inlet and outlet temperature of the sink and source are provided as the boundary condition for the HTHP cycle.

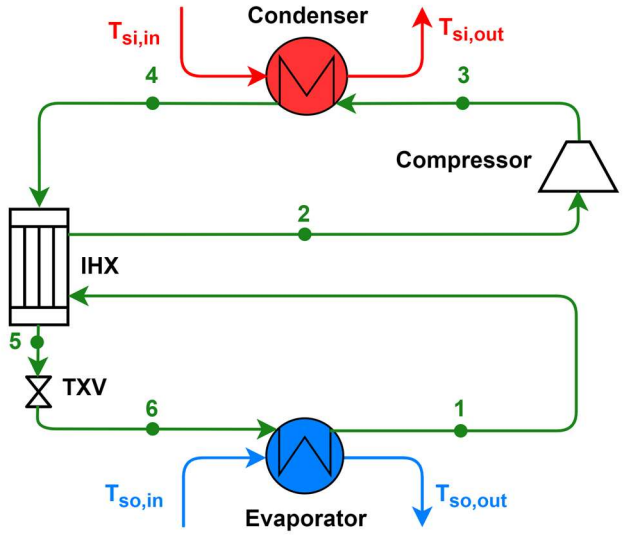

Figure 2. Schematic diagram of the HTHP cycle and its main components.

An optimization framework was developed to find the maximum achievable COP for each refrigerant mixture at a given sink/source temperature profile. Five process parameters were optimized: superheat at the evaporator (ΔT_{sh}), subcooling at the condenser (ΔT_{sc}), pressure at the evaporator (p_{ev}), pressure at the condenser (p_{cd}), and mole fraction of the first component in the binary mixture (z_1). The basinhopping global optimizer implemented in the Python SciPy library [25] was used as the optimization algorithm. Three soft constraints were considered in the optimization framework. The first and second constraints set the pinch point temperature difference at the condenser (i.e. $PPTD_{cd}$) and the pinch point temperature difference at the evaporator (i.e. $PPTD_{ev}$) equal to 5°C, which is a typical value for large-scale heat pumps [26]. The third constraint avoids wet compression. As long as these constraints are not met, the COP is divided by a factor (e.g. 10) to penalize the objective function.

3. Results and Discussion

3.1. Experimental *pvTz* measurements

3.1.1. Experimental Data

A summary of the ranges of pressures and temperatures for 103 *pvTz* measurements of R1234ze(Z)/acetone binary system (55 in the two-phase region and 48 in the superheated vapor region) and 110 *pvTz* measurements of R1234ze(Z)/isohexane binary system (48 in the two-phase region and 62 in the superheated vapor region) are reported in Table 2 and 3, respectively. These tables show also the overall experimental mole fractions and average specific volumes of the presented measurements. The two-phase and vapor-phase *pvTz* behaviors of the six series of R1234ze(Z)/acetone binary system and the six series of R1234ze(Z)/isohexane binary system are shown in Figure 3 and 4, respectively. From their *T-p* behaviors, it is possible to determine the measurements in the two-phase region and the ones in the

superheated vapor region. The experimental *pvTz* data of R1234ze(Z)/acetone and R1234ze(Z)/isohexane binary systems measured in the two-phase and superheated vapor regions are reported in Appendix (Table A1-A4).

Table 2. Overall experimental mole fractions of R1234ze(Z), z_1, ranges of temperatures, ΔT, and pressures, Δp, and average specific volumes, v, for R1234ze(Z)(1)/acetone(2) binary system.

Series	z_1	ΔT (°C)	Δp (bar)	v ($m^3 \cdot kg^{-1}$)
1	0.2261	30.00-115.00	0.58-4.56	0.088107
2	0.3831	30.00-110.00	0.67-2.13	0.177723
3	0.4081	30.00-115.00	0.78-4.29	0.083282
4	0.4765	30.00-110.00	0.75-2.07	0.172050
5	0.5137	30.00-110.00	0.86-2.66	0.129009
6	0.6653	30.00-105.00	1.06-2.52	0.124085

Table 3. Overall experimental mole fractions of R1234ze(Z), z_1, ranges of temperatures, ΔT, and pressures, Δp, and average specific volumes, v, for R1234ze(Z)(1)/isohexane(2) binary system.

Series	z_1	ΔT (°C)	Δp (bar)	v ($m^3 \cdot kg^{-1}$)
1	0.2568	40.00-117.50	1.32-4.67	0.065668
2	0.4615	25.00-110.00	0.87-1.76	0.176018
3	0.5050	30.00-115.00	1.55-3.94	0.074817
4	0.5614	25.00-110.00	1.17-2.31	0.128567
5	0.5977	20.00-110.00	1.03-2.01	0.147668
6	0.7559	25.00-110.00	1.66-4.03	0.067940

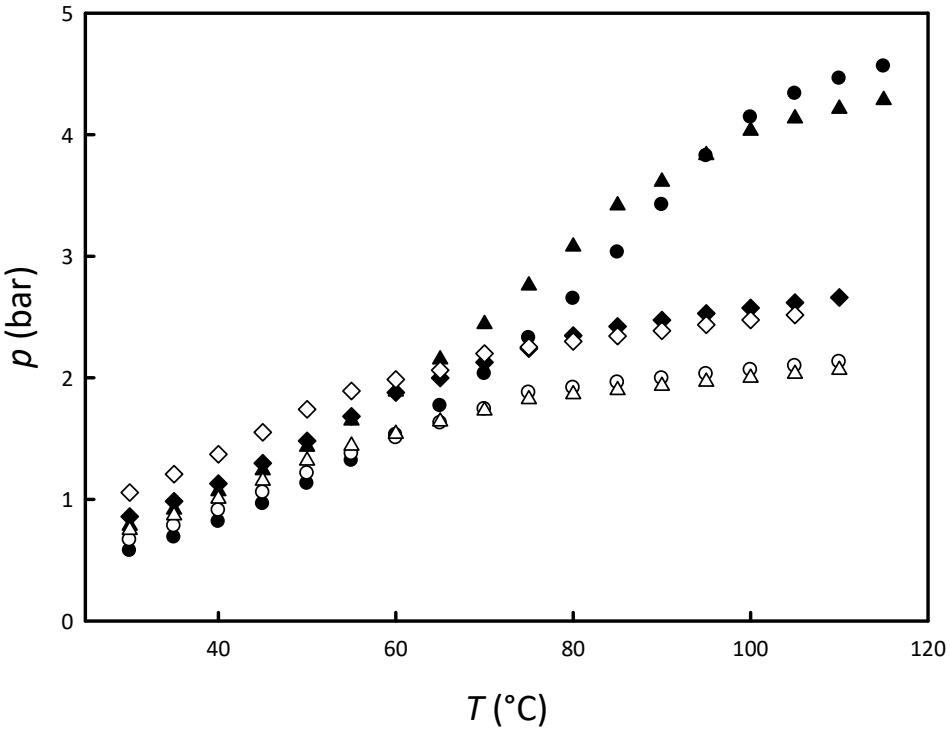

Figure 3. Two-phase and vapor-phase measurements of pressure, p, specific volume, v, temperature, T, and overall experimental mole fraction of R1234ze(Z), z_1 (Tables 5 and 6) for six isochores of R1234ze(Z)(1)/acetone(2) binary system; ●, series 1 (z_1 = 0.2261 and v = 0.088107 $m^3 \cdot kg^{-1}$); ○, series 2 (z_1 = 0.3831 and v = 0.177723 $m^3 \cdot kg^{-1}$); ▲, series 3 (z_1 = 0.4081 and v = 0.083282 $m^3 \cdot kg^{-1}$) Δ, series 4 (z_1 = 0.4765 and v = 0.172050 $m^3 \cdot kg^{-1}$); ◆, series 5 (z_1 = 0.5137 and v = 0.129009 $m^3 \cdot kg^{-1}$); ◇, series 6 (z_1 = 0.6653 and v = 0.124085 $m^3 \cdot kg^{-1}$).

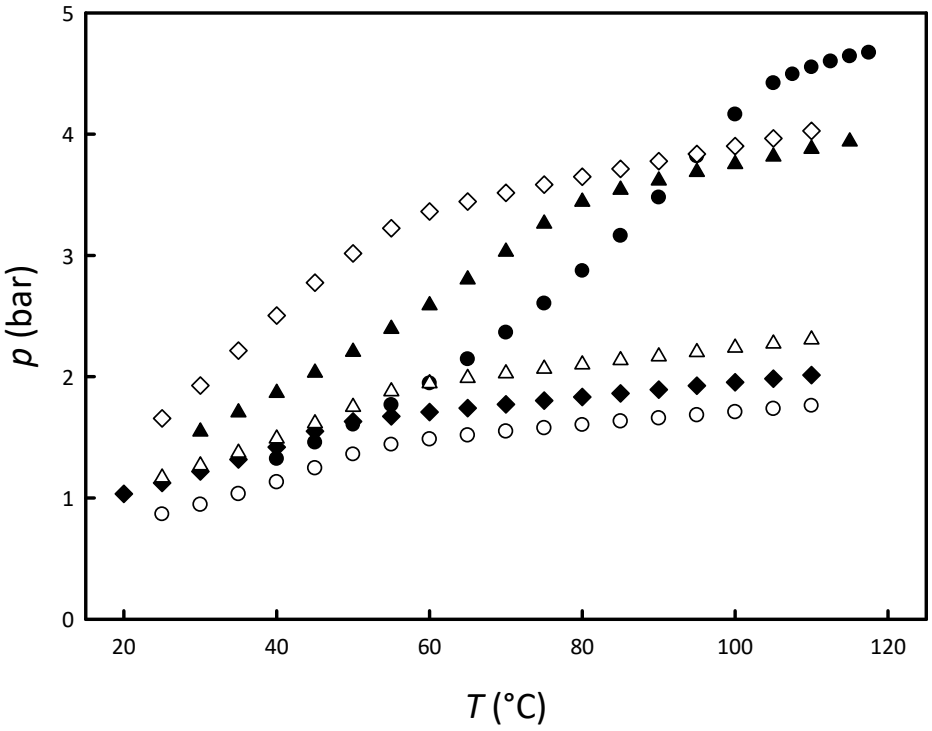

Figure 4. Two-phase and vapor-phase measurements of pressure, p, specific volume, v, temperature, T, and overall experimental mole fraction of R1234ze(Z), z_1 (Tables 7 and 8) for six isochores of R1234ze(Z)(1)/isohexane(2) binary system; ●, series 1 (z_1 = 0.2568 and v = 0.065668 $m^3 \cdot kg^{-1}$); ○, series 2 (z_1 = 0.4615 and v = 0.176018 $m^3 \cdot kg^{-1}$); ▲, series 3 (z_1 = 0.5050 and v = 0.074817 $m^3 \cdot kg^{-1}$); Δ, series 4 (z_1 = 0.5614 and v = 0.128567 $m^3 \cdot kg^{-1}$); ◆, series 5 (z_1 = 0.5977 and v = 0.147668 $m^3 \cdot kg^{-1}$); ◇, series 6 (z_1 = 0.7559 and v = 0.067940 $m^3 \cdot kg^{-1}$).

3.1.2. Assessment of the vapor-liquid equilibrium behavior

The VLE properties of R1234ze(Z)/acetone and R1234ze(Z)/isohexane binary systems derived from the two-phase measurements by using the "flash method" with the multi-fluid Helmholtz-energy explicit model are reported in Table 4 and 5, respectively. Both the estimated BIPs available in REFPROP 10.0 and the fitted BIPs were used in the simulations. These parameters are reported in Table 6. It should be noted that the points close to the superheated vapor region (highlighted in Table A2 and A4 in the appendix) were not used in the tuning. In fact, their pressure behavior is different from that of the other two-phase experimental points.

Table 4. Pressures, p_{calc}, and mole fractions of the liquid, x_1, and vapor, y_1, phases of R1234ze(Z) derived from the two-phase measurements of R1234ze(Z)(1)/acetone(2) binary system (Table A1 in the appendix) by using the "flash method" with the multi-fluid Helmholtz-energy explicit model.

	Model with estimated BIPs			Model with fitted BIPs		
T (°C)	p_{calc} (bar)	x_1	y_1	p_{calc} (bar)	x_1	y_1
z_1 = 0.2261						

	Model with estimated BIPs			Model with fitted BIPs		
T (°C)	p_{calc} (bar)	x_1	y_1	p_{calc} (bar)	x_1	y_1
30.00	0.70	0.1609	0.5308	0.57	0.1860	0.4631
35.00	0.82	0.1541	0.5061	0.69	0.1811	0.4444
40.00	0.95	0.1472	0.4811	0.81	0.1760	0.4257
45.00	1.11	0.1404	0.4561	0.96	0.1708	0.4071
50.00	1.28	0.1336	0.4311	1.13	0.1654	0.3886
55.00	1.47	0.1270	0.4065	1.31	0.1600	0.3702
60.00	1.69	0.1206	0.3823	1.52	0.1546	0.3522
65.00	1.93	0.1143	0.3588	1.76	0.1491	0.3346
70.00	2.20	0.1084	0.3360	2.02	0.1437	0.3175
75.00	2.49	0.1027	0.3142	2.32	0.1383	0.3008
80.00	2.82	0.0973	0.2934	2.65	0.1330	0.2847
85.00	3.19	0.0922	0.2736	3.01	0.1279	0.2693
90.00	3.59	0.0874	0.2549	3.41	0.1228	0.2544
z_1 = 0.3831						
30.00	0.78	0.2054	0.5992	0.67	0.2572	0.5831
35.00	0.90	0.1905	0.5657	0.78	0.2448	0.5543
40.00	1.03	0.1763	0.5317	0.91	0.2325	0.5250
45.00	1.17	0.1630	0.4975	1.06	0.2204	0.4958
50.00	1.34	0.1506	0.4638	1.22	0.2086	0.4668
55.00	1.52	0.1391	0.4309	1.41	0.1972	0.4384
z_1 = 0.4081						
30.00	0.95	0.3021	0.7057	0.78	0.3327	0.6840
35.00	1.10	0.2895	0.6834	0.92	0.3234	0.6634
40.00	1.27	0.2764	0.6598	1.07	0.3138	0.6420
45.00	1.45	0.2632	0.6351	1.24	0.3038	0.6198
50.00	1.66	0.2500	0.6093	1.43	0.2936	0.5970
55.00	1.88	0.2370	0.5827	1.64	0.2833	0.5738
60.00	2.13	0.2242	0.5556	1.88	0.2729	0.5502
65.00	2.40	0.2118	0.5282	2.14	0.2626	0.5266
70.00	2.69	0.2000	0.5008	2.43	0.2524	0.5029
75.00	3.01	0.1886	0.4736	2.75	0.2423	0.4795
80.00	3.37	0.1779	0.4468	3.10	0.2325	0.4564
z_1 = 0.4765						
30.00	0.88	0.2625	0.6674	0.76	0.3186	0.6669
35.00	1.01	0.2429	0.6344	0.88	0.3027	0.6372
40.00	1.14	0.2242	0.6001	1.02	0.2870	0.6066
45.00	1.30	0.2066	0.5651	1.17	0.2716	0.5754
50.00	1.47	0.1902	0.5299	1.34	0.2566	0.5440
z_1 = 0.5137						
30.00	1.00	0.3296	0.7289	0.85	0.3750	0.7304
35.00	1.14	0.3090	0.7014	0.98	0.3593	0.7049

	Model with estimated BIPs			Model with fitted BIPs		
T (°C)	p_{calc} (bar)	x_1	y_1	p_{calc} (bar)	x_1	y_1
40.00	1.30	0.2886	0.6720	1.13	0.3434	0.6781
45.00	1.47	0.2688	0.6411	1.30	0.3276	0.6501
50.00	1.66	0.2498	0.6091	1.48	0.3119	0.6212
55.00	1.86	0.2319	0.5764	1.68	0.2965	0.5919
60.00	2.09	0.2151	0.5434	1.91	0.2814	0.5623
z_1 = 0.6653						
30.00	1.20	0.4532	0.8109	1.05	0.4910	0.8293
35.00	1.37	0.4242	0.7862	1.20	0.4691	0.8062
40.00	1.54	0.3948	0.7587	1.37	0.4469	0.7808
45.00	1.73	0.3660	0.7289	1.55	0.4247	0.7535
50.00	1.93	0.3382	0.6971	1.74	0.4028	0.7244

Table 5. Pressures, p_{calc}, and mole fractions of the liquid, x_1, and vapor, y_1, phases of R1234ze(Z) derived from the two-phase measurements of R1234ze(Z)(1)/isohexane(2) binary system (Table A3 in the appendix) by using the "flash method" with the multi-fluid Helmholtz-energy explicit model.

	Model with estimated BIPs			Model with fitted BIPs		
T (°C)	p_{calc} (bar)	x_1	y_1	p_{calc} (bar)	x_1	y_1
z_1 = 0.2568						
40.00	1.06	0.1472	0.5733	1.31	0.0839	0.6265
45.00	1.21	0.1387	0.5465	1.45	0.0775	0.5927
50.00	1.37	0.1306	0.5192	1.60	0.0718	0.5586
55.00	1.55	0.1228	0.4918	1.76	0.0667	0.5247
60.00	1.74	0.1155	0.4645	1.94	0.0622	0.4913
65.00	1.95	0.1085	0.4376	2.14	0.0581	0.4587
70.00	2.18	0.1020	0.4112	2.37	0.0544	0.4272
75.00	2.44	0.0960	0.3856	2.61	0.0511	0.3971
80.00	2.71	0.0904	0.3610	2.88	0.0481	0.3684
85.00	3.02	0.0851	0.3373	3.17	0.0455	0.3412
90.00	3.35	0.0803	0.3148	3.49	0.0430	0.3157
95.00	3.71	0.0759	0.2934	3.85	0.0408	0.2918
z_1 = 0.4615						
25.00	0.75	0.2005	0.6802	0.86	0.0870	0.6862
30.00	0.84	0.1804	0.6452	0.94	0.0773	0.6464
35.00	0.95	0.1623	0.6089	1.03	0.0693	0.6059
40.00	1.06	0.1462	0.5718	1.14	0.0625	0.5652
45.00	1.18	0.1321	0.5346	1.25	0.0568	0.5250
50.00	1.32	0.1196	0.4978	1.38	0.0518	0.4858
z_1 = 0.5050						
30.00	1.17	0.3500	0.7795	1.55	0.2253	0.8008

	Model with estimated BIPs			Model with fitted BIPs		
T (°C)	p_{calc} (bar)	x_1	y_1	p_{calc} (bar)	x_1	y_1
35.00	1.33	0.3299	0.7598	1.71	0.1995	0.7768
40.00	1.51	0.3093	0.7381	1.87	0.1774	0.7502
45.00	1.69	0.2888	0.7145	2.03	0.1588	0.7215
50.00	1.89	0.2687	0.6891	2.21	0.1430	0.6911
55.00	2.10	0.2495	0.6622	2.39	0.1297	0.6596
60.00	2.33	0.2313	0.6341	2.59	0.1183	0.6272
65.00	2.57	0.2144	0.6052	2.81	0.1085	0.5946
70.00	2.82	0.1987	0.5758	3.04	0.1001	0.5620
z_1 = 0.5614						
25.00	0.95	0.3268	0.7754	1.17	0.1631	0.7788
30.00	1.08	0.2981	0.7492	1.27	0.1416	0.7472
35.00	1.21	0.2706	0.7203	1.38	0.1244	0.7133
40.00	1.35	0.2450	0.6893	1.50	0.1105	0.6779
45.00	1.49	0.2216	0.6565	1.63	0.0990	0.6415
50.00	1.65	0.2007	0.6225	1.77	0.0894	0.6047
z_1 = 0.5977						
20.00	0.84	0.3587	0.8001	1.04	0.1766	0.8002
25.00	0.95	0.3254	0.7746	1.13	0.1505	0.7691
30.00	1.07	0.2932	0.7460	1.22	0.1303	0.7354
35.00	1.19	0.2633	0.7147	1.32	0.1144	0.6998
40.00	1.32	0.2361	0.6813	1.44	0.1016	0.6629
45.00	1.46	0.2120	0.6464	1.56	0.0910	0.6252
z_1 = 0.7559						
25.00	1.36	0.6533	0.8981	1.65	0.6365	0.8684
30.00	1.58	0.6324	0.8881	1.92	0.5997	0.8610
35.00	1.82	0.6079	0.8763	2.22	0.5479	0.8513
40.00	2.07	0.5798	0.8624	2.52	0.4774	0.8377

Table 6. Estimated and fitted BIPs of multi-fluid Helmholtz-energy explicit model for the selected mixtures.

mixture	BIP	$\beta_{T,ij}$	$\beta_{v,ij}$	$\gamma_{T,ij}$	$\gamma_{v,ij}$
R1234ze(Z)/acetone	Estimated	1	1	0.99667	1.0022
	Fitted	0.998808	1	1.031785	1
R1234ze(Z)/isohexane	Estimated	1	1	0.97058	1.0125
	Fitted	1.008428	1	0.916539	1

As shown in Figure 5, the estimated BIPs provided higher pressure deviations for R1234ze(Z)/acetone binary system than that given by the fitted BIPs. In fact, the model with the estimated BIPs always overestimated the two-phase pressures of this mixture, providing deviations also higher that 20 % for some series and AARD (p) = 13.05 %. Instead, the model with the fitted BIPs ensured an AARD (p) of 0.49 % and pressure deviations between ±1 % for most of the experimental points.

Figure 6 shows that, also for R1234ze(Z)/isohexane binary system, the pressure deviations given by the model with the estimated BIPs were higher than that obtained by the fitted BIPs. However, in this case, the two-phase pressures obtained from the estimated BIPs were highly underestimated, yielding deviations also higher that 20 % for some series and an AARD (p) of 11.69 %. More accurate results were provided by the model with the fitted BIPs, ensuring AARD (p) = 0.42 %.

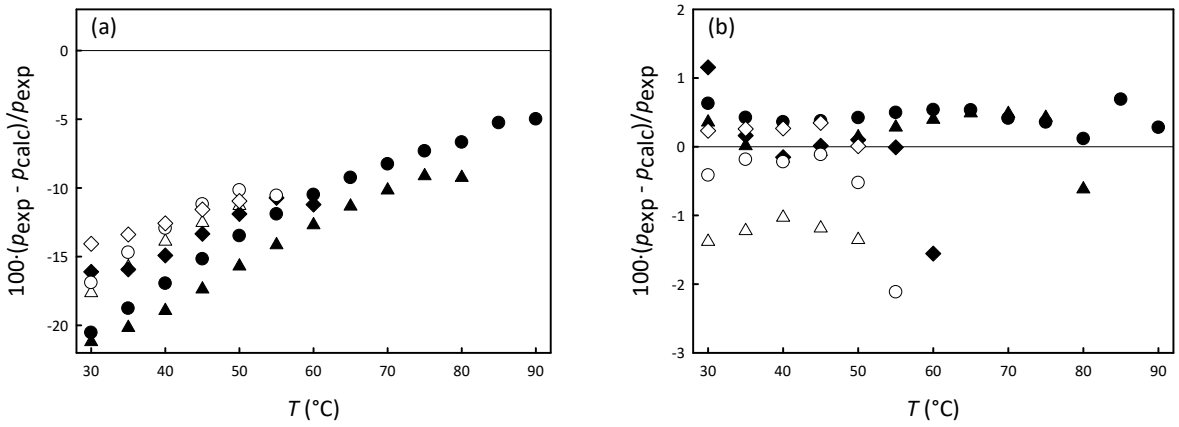

Figure 5. Deviations between the pressures, p_{exp}, for R1234ze(Z)(1)/acetone(2) binary system measured in the two phase region (Table A1 in the appendix) and pressures, p_{calc}, calculated from the multi-fluid Helmholtz-energy explicit model using the estimated BIPs available in REFPROP 10.0 (a) and the multi-fluid Helmholtz-energy explicit model using the fitted BIPs (b); ●, series 1 (z_1 = 0.2261 and v = 0.088107 $m^3 \cdot kg^{-1}$); ○, series 2 (z_1 = 0.3831 and v = 0.177723 $m^3 \cdot kg^{-1}$); ▲, series 3 (z_1 = 0.4081 and v = 0.083282 $m^3 \cdot kg^{-1}$) Δ, series 4 (z_1 = 0.4765 and v = 0.172050 $m^3 \cdot kg^{-1}$); ◆, series 5 (z_1 = 0.5137 and v = 0.129009 $m^3 \cdot kg^{-1}$); ◇, series 6 (z_1 = 0.6653 and v = 0.124085 $m^3 \cdot kg^{-1}$).

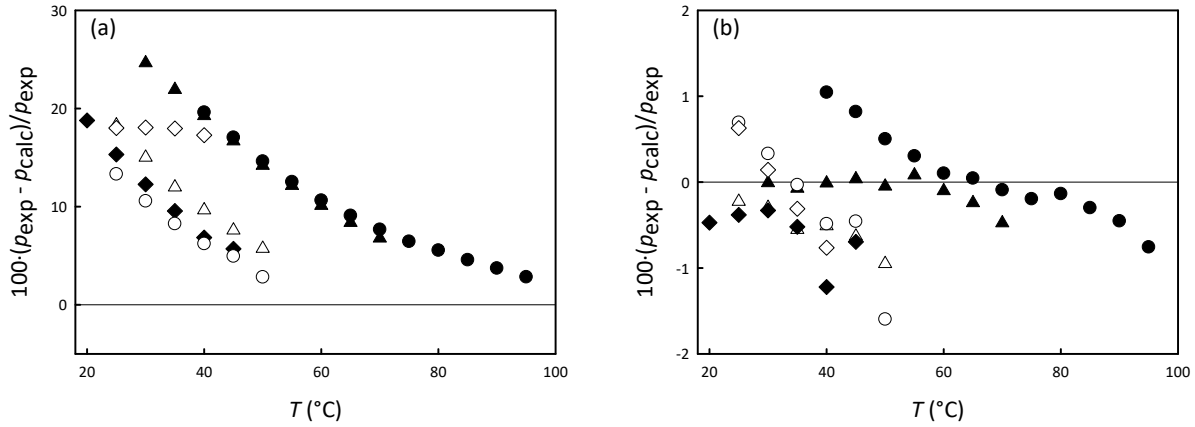

Figure 6. Deviations between the pressures, p_{exp}, for R1234ze(Z)(1)/isohexane(2) binary system measured in the two phase region (Table A3 in the appendix) and pressures, p_{calc}, calculated from the multi-fluid Helmholtz-energy explicit model using the estimated BIPs available in REFPROP 10.0 (a) and the multi-fluid Helmholtz-energy explicit model using the fitted BIPs (b); ●, series 1 (z_1 = 0.2568 and v = 0.065668 $m^3 \cdot kg^{-1}$); ○, series 2 (z_1 = 0.4615 and v = 0.176018 $m^3 \cdot kg^{-1}$); ▲, series 3 (z_1 = 0.5050 and v = 0.074817 $m^3 \cdot kg^{-1}$); Δ, series 4 (z_1 = 0.5614 and v = 0.128567 $m^3 \cdot kg^{-1}$); ◆, series 5 (z_1 = 0.5977 and v = 0.147668 $m^3 \cdot kg^{-1}$); ◇, series 6 (z_1 = 0.7559 and v = 0.067940 $m^3 \cdot kg^{-1}$).

3.1.3. Vapor-phase pvTz

The vapor-phase experimental data of R1234ze(Z)/acetone and R1234ze(Z)/isohexane binary systems were compared with the calculations provided by the multi-fluid Helmholtz-energy explicit model using both the estimated BIPs of REFPROP 10.0 and the fitted BIPs (reported in Table 6). Again, since they showed a different pressure behavior with respect to the other vapor-phase data, the points close to the two-phase region highlighted in Table A2 and A4 in the Appendix were not used in the calculations.

The deviations between the experimental pressures of the two binary systems and the data provided by the selected models are shown in

Figure 7 and 8. As evident in

Figure 7, the models always overestimated the vapor-phase pressures of R1234ze(Z)/acetone binary system, but the deviations were between ±3 % for most of the experimental points. An AARD (p) of 1.55 % was obtained by comparing the experimental pressures of this mixture and the values calculated by using the estimated BIPs of REFPROP 10.0. The multi-fluid Helmholtz-energy explicit model with the BIPs tuned to the two-phase *pvTz* measurements of this mixture provided an AARD (p) of 1.24 %.

Figure 8 shows that the models ensured more accurate results for R1234ze(Z)/isohexane binary system, yielding pressure deviations between ±3 % for almost all the points. In particular, the deviations given by the model with the estimated BIPs (AARD (p) = 0.24 %) were slightly lower than those provided by the model with the fitted BIPs (AARD (p) = 0.67 %).

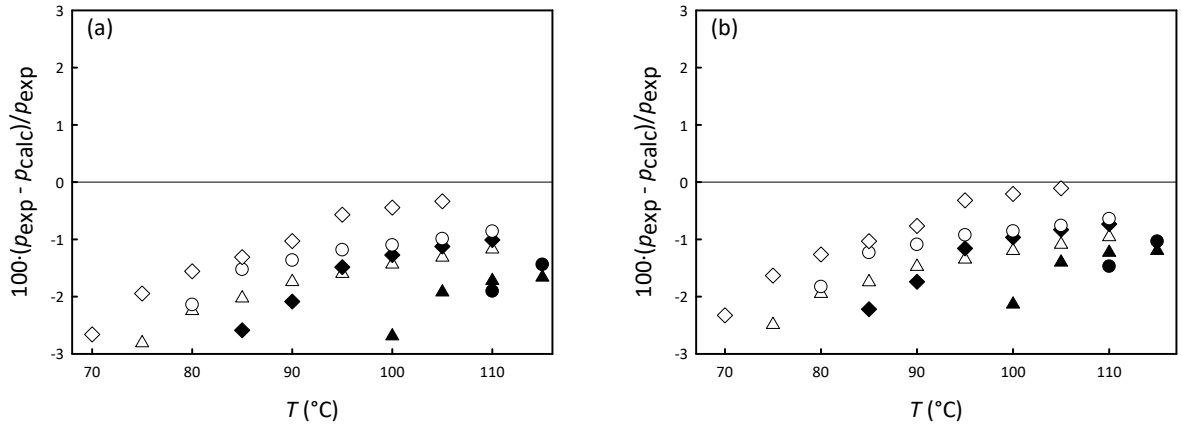

Figure 7. Deviations between the pressures, p_{exp}, of R1234ze(Z)(1)/acetone(2) binary system measured in the superheated vapor region (Table A2 in the appendix) and the pressures, p_{calc}, calculated with the multi-fluid Helmholtz-energy explicit model using the estimated BIPs available in REFPROP 10.0 (a) and the multi-fluid Helmholtz-energy explicit model using the fitted BIPs (b); ●, series 1 (z_1 = 0.2261 and v = 0.088107 $m^3 \cdot kg^{-1}$); ○, series 2 (z_1 = 0.3831 and v = 0.177723 $m^3 \cdot kg^{-1}$); ▲, series 3 (z_1 = 0.4081 and v = 0.083282 $m^3 \cdot kg^{-1}$) Δ, series 4 (z_1 = 0.4765 and v = 0.172050 $m^3 \cdot kg^{-1}$); ◆, series 5 (z_1 = 0.5137 and v = 0.129009 $m^3 \cdot kg^{-1}$); ◇, series 6 (z_1 = 0.6653 and v = 0.124085 $m^3 \cdot kg^{-1}$).

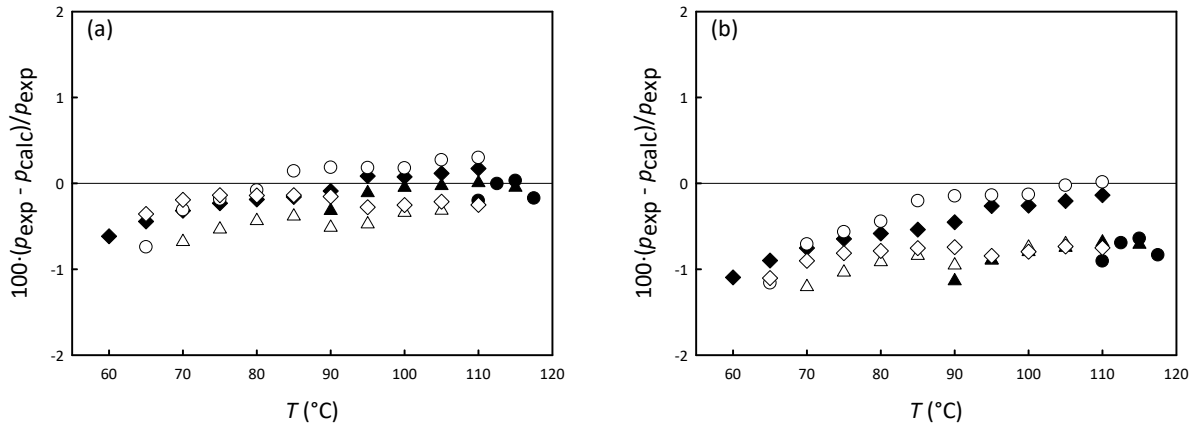

Figure 8. Deviations between the pressures, p_{exp}, of R1234ze(Z)(1)/isohexane(2) binary system measured in the superheated vapor region (Table A4 in the appendix) and the pressures, p_{calc}, calculated with the multi-fluid Helmholtz-energy explicit model using the estimated BIPs available in REFPROP 10.0 (a) and the multi-fluid Helmholtz-energy explicit model using the fitted BIPs (b); ●, series 1 (z_1 = 0.2568 and v = 0.065668 $m^3 \cdot kg^{-1}$); ○, series 2 (z_1 = 0.4615 and v = 0.176018 $m^3 \cdot kg^{-1}$); ▲, series 3 (z_1 = 0.5050 and v = 0.074817 $m^3 \cdot kg^{-1}$); Δ, series 4 (z_1 = 0.5614 and v = 0.128567 $m^3 \cdot kg^{-1}$); ◆, series 5 (z_1 = 0.5977 and v = 0.147668 $m^3 \cdot kg^{-1}$); ◇, series 6 (z_1 = 0.7559 and v = 0.067940 $m^3 \cdot kg^{-1}$).

3.2. Temperature glide of the mixtures using estimated and fitted BIPs

Phase-change temperature glide of R1234ze(Z)/acetone and R1234ze(Z)/isohexane at various pressures and compositions using estimated and fitted BIPs are shown in Figure 9 and 10, respectively. For both mixtures by increasing the pressure the temperature glide was reduced, using either estimated or fitted BIPs. For R1234ze(Z)/acetone the range of temperature glides using estimated and fitted BIPs are similar. However, the optimum composition to achieve the highest temperature glide was changed significantly once fitted BIPs are used. On the other hand, for R1234ze(Z)/isohexane, the temperature glides increased significantly once fitted BIPs are used. But the optimum composition to reach the highest temperature glide did not change significantly. For both mixtures, the optimum composition corresponding to the highest temperature glide was quite similar for different pressures, either using estimated or fitted BIPs. Overall, for both mixtures, phase change behavior was changed significantly once BIPs are fitted based on experimental isochoric data.

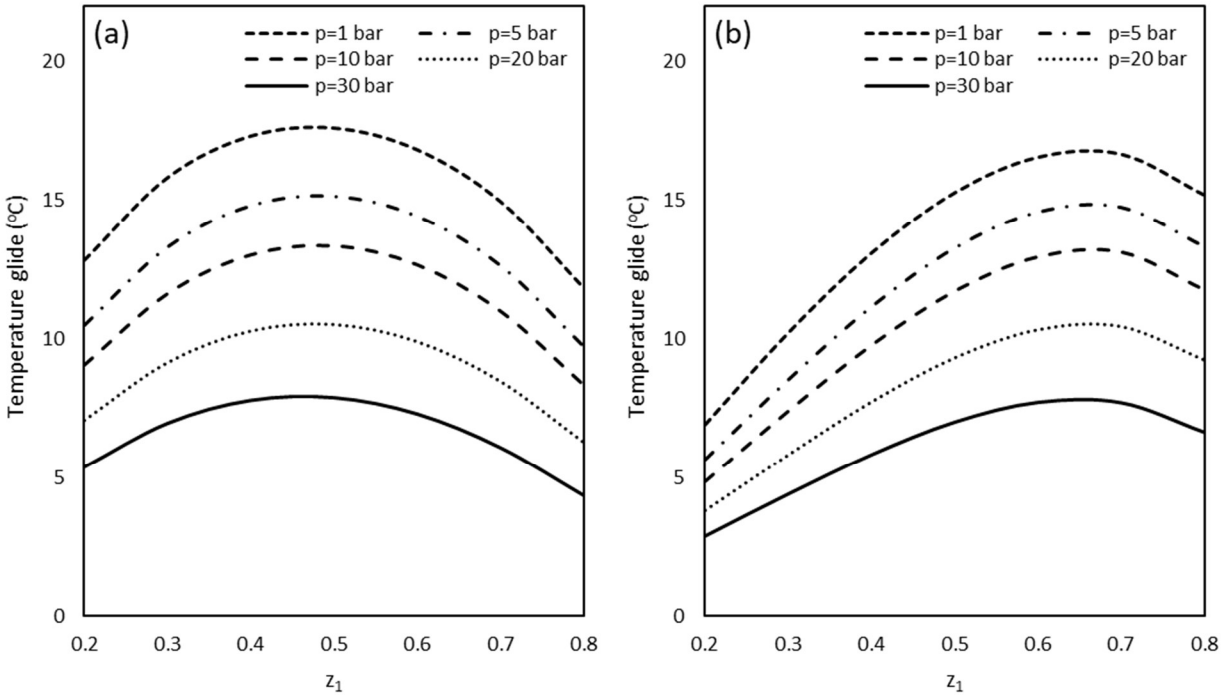

Figure 9. Phase-change temperature glide of R1234ze(Z)/acetone versus composition at different pressures using (a) estimated BIPs and (b) fitted BIPs.

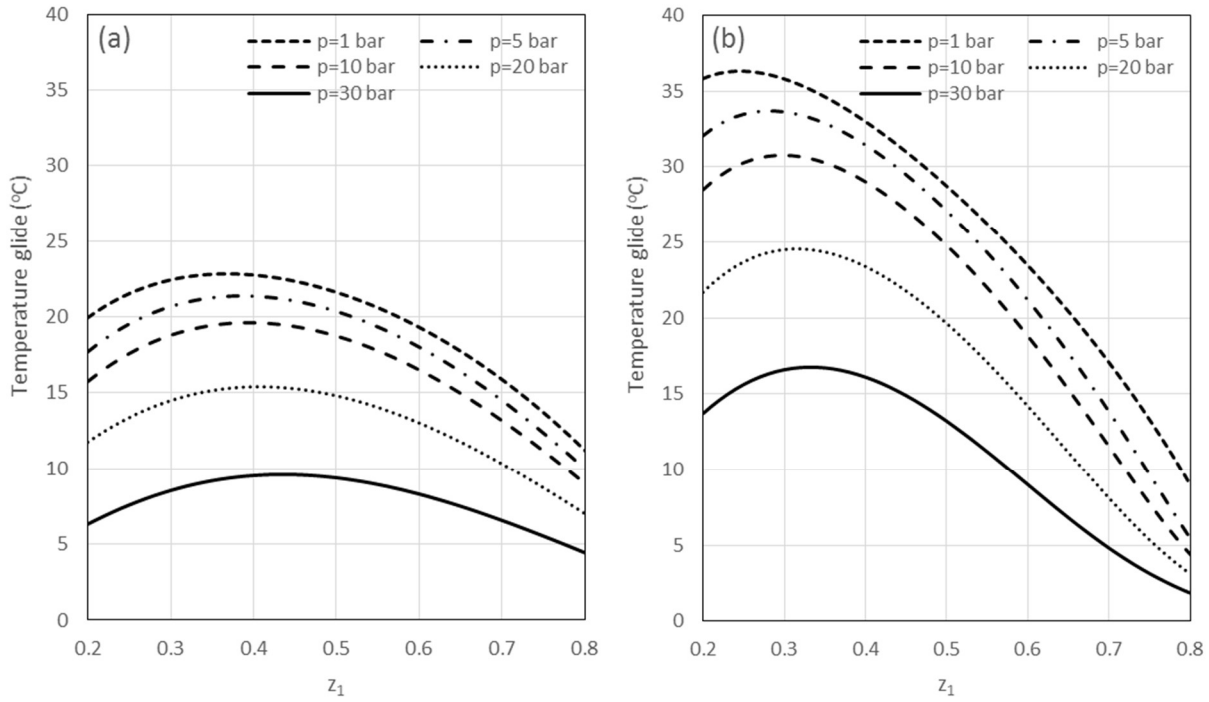

Figure 10. Phase-change temperature glide of R1234ze(Z)/isohexane versus composition at different pressures using (a) estimated BIPs and (b) fitted BIPs.

3.3. Cycle optimization results using estimated and fitted BIPs

In this section, HTHP cycle was optimized for the two zeotropic mixtures, once with estimated BIPs and once with fitted BIPs. The following boundary conditions were considered for the cycle optimization: $T_{si,in}$ =140 °C, $T_{si,out}$ =200 °C, $T_{so,in}$ =120 °C, $T_{so,out}$ =100 °C. $PPTD_{ev}$ and $PPTD_{cd}$ were set to 5 °C. T-H diagram for the R1234ze(Z)/acetone and R1234ze(Z)/isohexane are shown in Figure 11 and 12, respectively, while their main cycle properties are reported in Table 7. The COP obtained with R1234ze(Z)/acetone was higher than that of R1234ze(Z)/isohexane. For R1234ze(Z)/acetone the COP was slightly reduced by around 0.25% once BIPs are fitted. However, z_1 significantly changed once fitted BIPs are used. This agrees with phase change temperature glide curve of this mixture (Figure 9). According to that figure, by tuning the BIPs, the optimum mole fraction to reach the highest temperature glide changed significantly, while the range of temperature glide did not change that much. By tuning the BIPs, the superheating in the evaporator was increased, while the subcooling in the condenser was decreased. Compared to the case with estimated BIPs, both the evaporator and condenser's pressures were slightly increased once the BIPs are fitted.

For R1234ze(Z)/isohexane with fitted BIPs, COP was around 1.7% lower than the COP obtained by estimated BIPs. This is in agreement with Figure 10 where the phase change temperature glide of this mixture changed significantly by tuning the BIPs.

Table 7. Comparison of the optimized cycle properties of the VHTHP cycle using estimated and fitted BIPs.

Mixture	BIP	P_{ev} (bar)	P_{cd} (bar)	ΔT_{sh} (°C)	ΔT_{sc} (°C)	z_1	COP	VHC (kJ m^{-3})	$T_{c,out}$ (°C)	$T_{g,cd}$ (°C)	$T_{g,ev}$ (°C)
R1234ze(z)/acetone	Estimated	7.0	35.9	2.5	36.5	0.48	3.95	5815	224.4	6.2	11.2
	Fitted	7.9	38.8	9.2	31.9	0.68	3.94	6308	221.8	5.9	10.7
R1234ze(z)/isohexane	Estimated	6.9	35.7	0.0	43.5	0.48	3.90	5216	207.0	0.0	14.7
	Fitted	9.3	43.1	4.4	37.1	0.57	3.83	6443	207.1	0.0	15.6

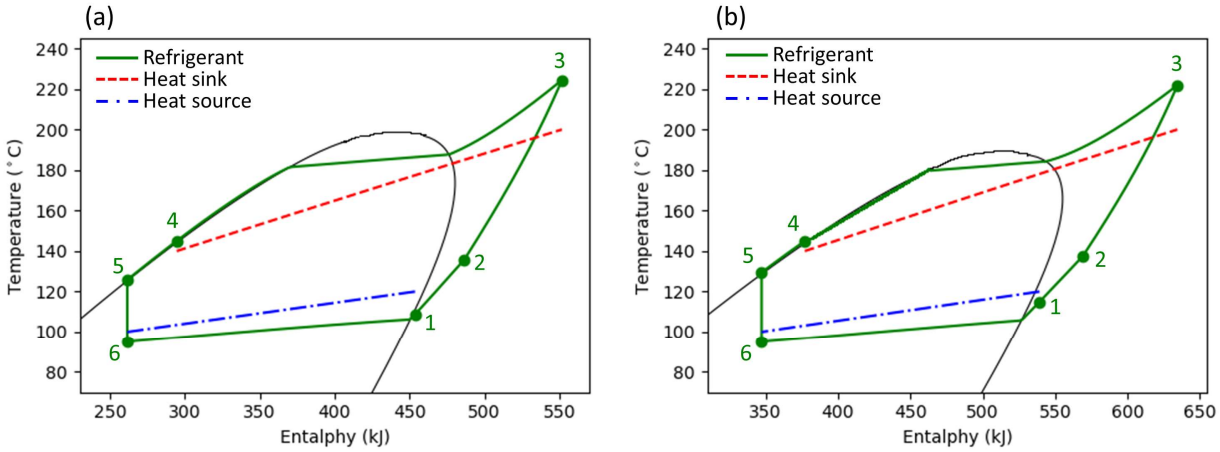

Figure 11. T-H diagrams of the VHTHP cycle working with R1234ze(Z)/acetone using (a) estimated BIPs and (b) fitted BIPs.

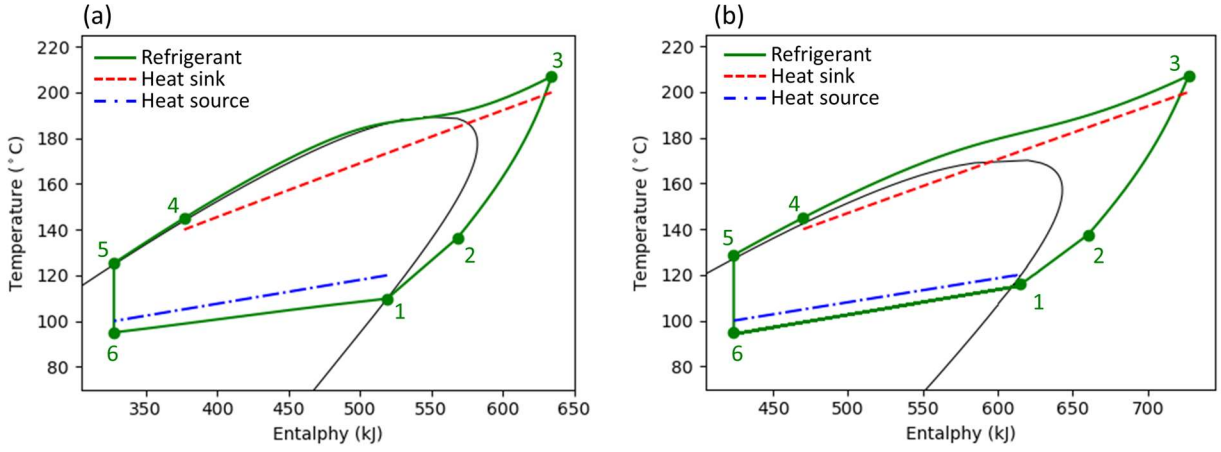

Figure 12. T-H diagrams of the VHTHP cycle working with R1234ze(Z)/isohexane using (a) estimated BIPs and (b) fitted BIPs.

3.4. Sensitivity analysis

Sensitivity analysis was performed to study the effect of variation in pinch-point temperature difference, heat sink temperature glide and heat source temperature glide on the heat pump simulation results. This analysis can show how tuning BIPs will influence the performance of VHTHP at different conditions.

3.4.1. Effect of changing pinch point temperature difference

Effect of changing pinch-point temperature difference (both $PPTD_{ev}$ and $PPTD_{cd}$) on the performance of HTHP working with R1234ze(Z)/acetone and R1234ze(Z)/isohexane are depicted on Figure 13 and 14, respectively. In all these simulations, the following boundary conditions were considered: $T_{si,in}$ =140 °C, $T_{si,out}$ =200 °C, $T_{so,in}$ =120 °C, $T_{so,out}$ =100 °C.

According to these results, for both mixtures the COP was reduced by increasing the PPTD, while the trends changed by changing the mixture due to its specific thermodynamic properties. Similar trend was reported by [26]. For R1234ze(Z)/acetone (Figure 13), the COP obtained using estimated and fitted BIPs are quite similar at various PPTDs. However, z_1 changed significantly once the BIPs are fitted. No specific trend between z_1 and PPTD was observed. For R1234ze(Z)/isohexane (Figure 14), there is a significant difference between COP obtained by estimated BIPs and fitted BIPs at different PPTDs. There is also a significant difference between z1 obtained by estimated and fitted BIPs. However this difference was reduced by decreasing the PPTD.

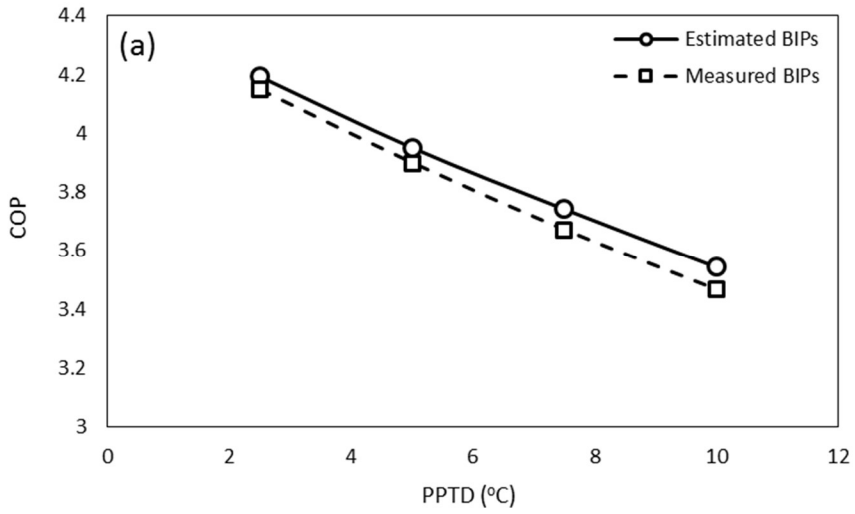

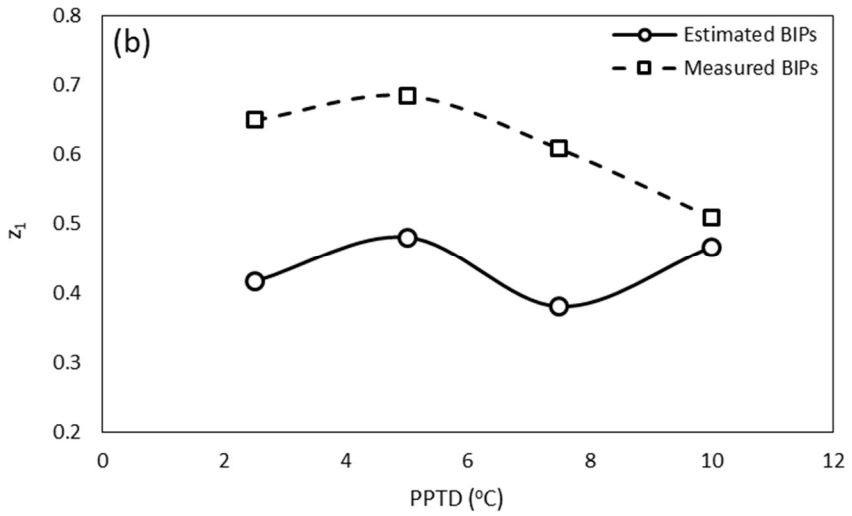

Figure 13. Effect of pinch point temperature on (a) COP and (b) z_1 for R1234ze(Z)/acetone with estimated and measured (fitted) BIPs.

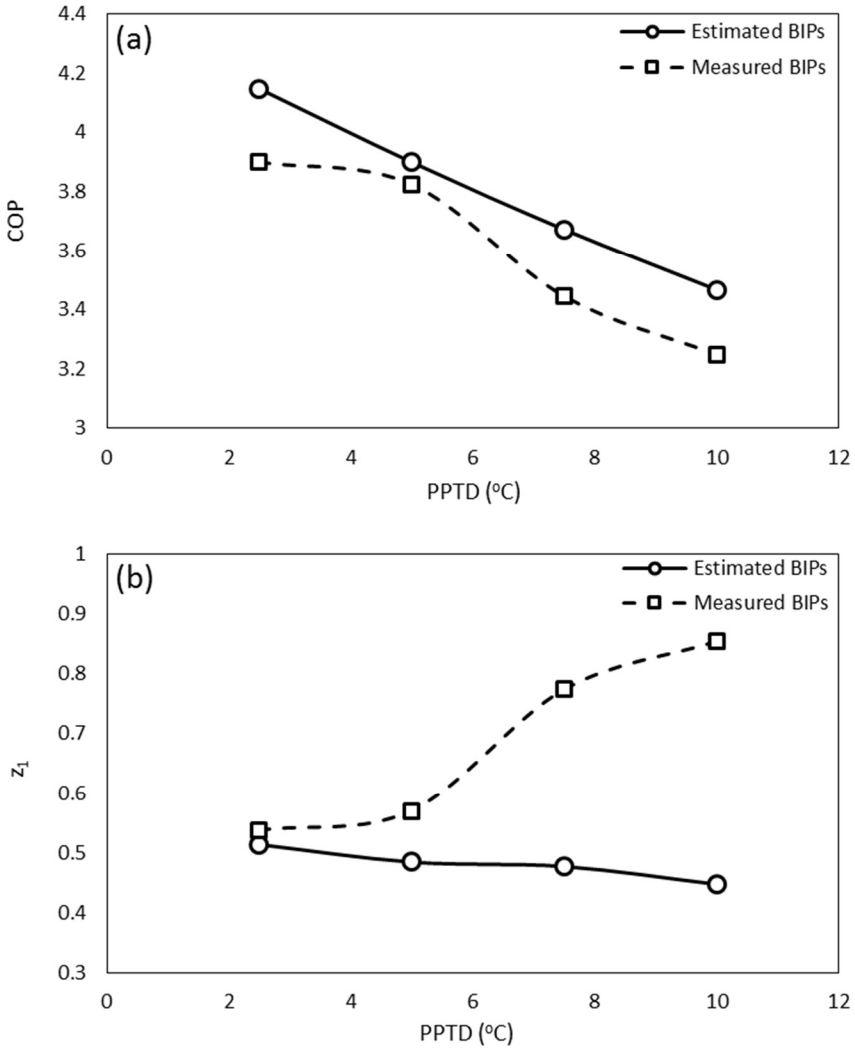

Figure 14. Effect of pinch point temperature on (a) COP and (b) z_1 for R1234ze(Z)/isohexane with estimated and measured (fitted) BIPs.

3.4.2. Effect of changing temperature glide in the heat sink

The effect of heat sink temperature glide variation on the performance of HTHP working with R1234ze(Z)/acetone and R1234ze(Z)/isohexane are depicted on Figure 15 and 16, respectively. In all these simulations $PPTD_{ev}$ and $PPTD_{cd}$ was 5 °C, $T_{si,out}$ was 200 °C, $T_{so,in}$ was 120 °C, and $T_{so,out}$ was 100 °C. $T_{si,in}$ varied to make different sink temperature glides.

For both mixtures, COP was increased by increasing the sink temperature glide. This is because by increasing the sink temperature glide, the temperature lift (difference between average sink temperature and average source temperature) is decreased. It was shown that by reducing the temperature lift, COP will increase [27]. For R1234ze(Z)/acetone (Figure 15), the COP obtained by estimated and fitted BIPs are quite similar. However, z_1 changed once the BIPs are fitted. For both estimated and fitted BIPs, z_1 was increased by increasing the sink temperature glide. For R1234ze(Z)/isohexane (Figure 16), there is a

significant difference between COP obtained by estimated and fitted BIPs at different sink temperature glides. There is also a significant difference between z_1 obtained by estimated and fitted BIPs.

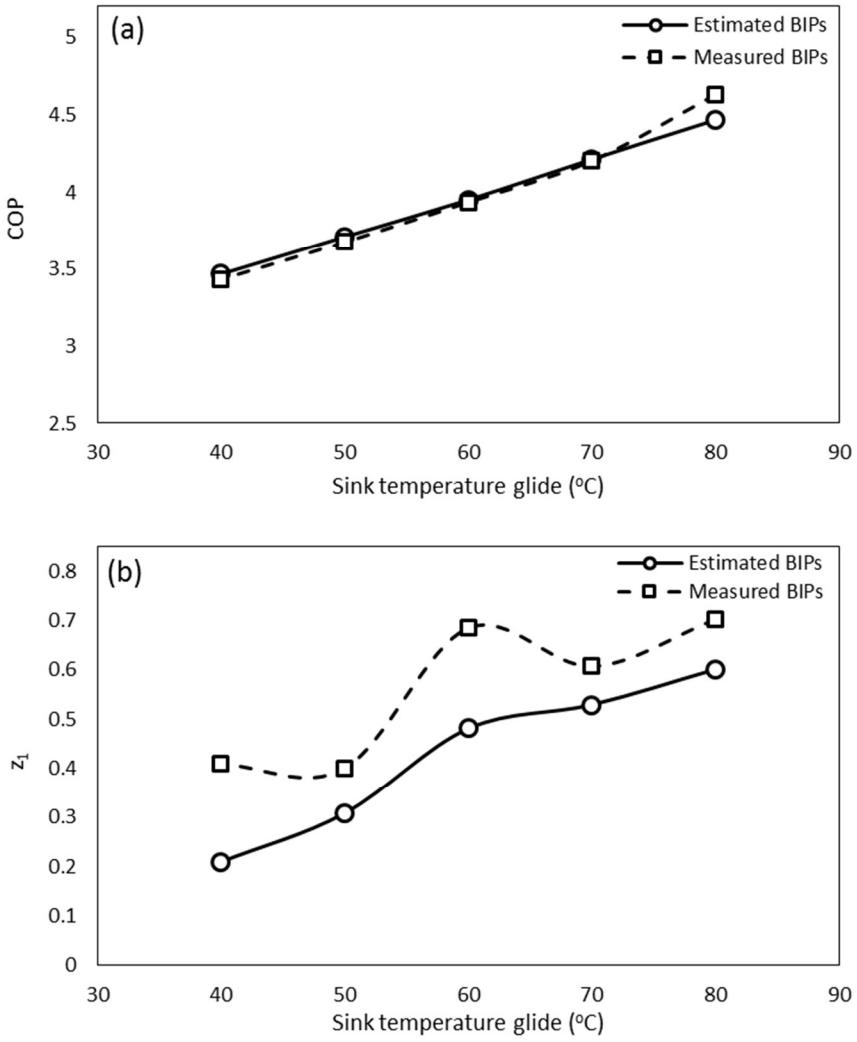

Figure 15. Effect of heat sink temperature glide on (a) COP and (b) z_1 for R1234ze(Z)/acetone with estimated and measured (fitted) BIPs.

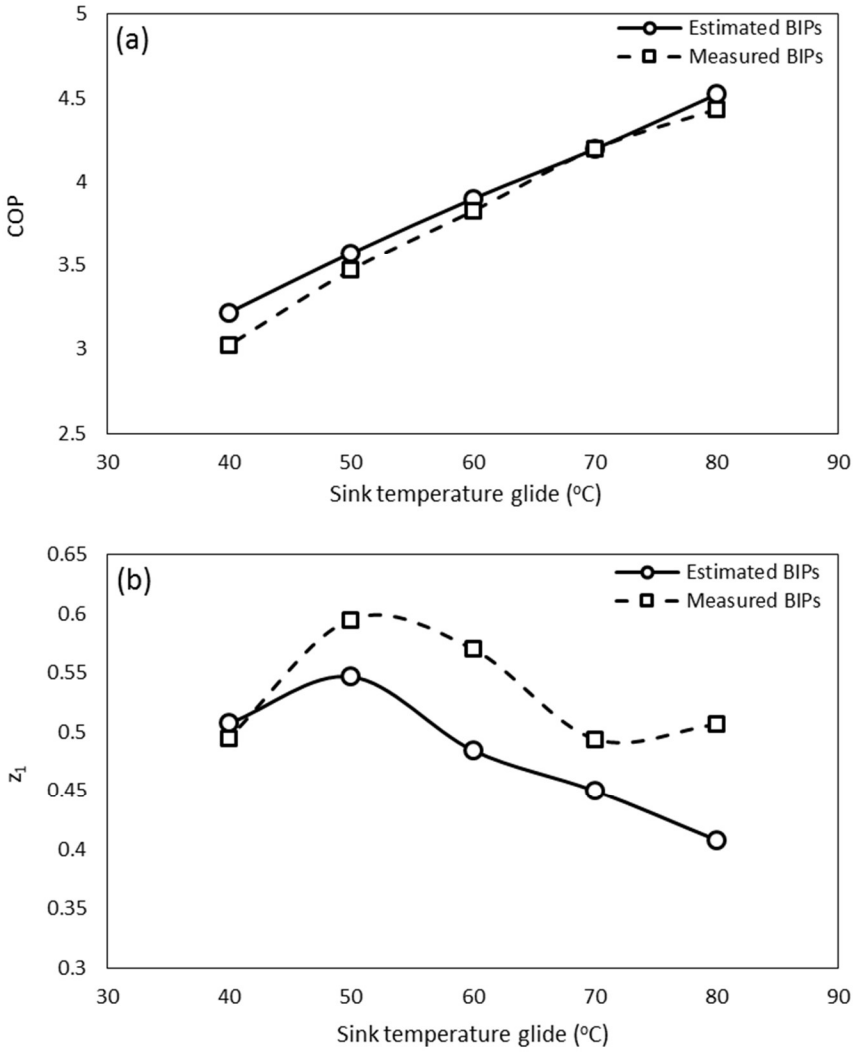

Figure 16. Effect of heat sink temperature glide on (a) COP and (b) z_1 for of R1234ze(Z)/isohexane with estimated and measured (fitted) BIPs.

3.4.3. Effect of changing temperature glide in the heat source

Effect of heat source temperature glide on the performance of HTHP working with R1234ze(Z)/acetone and R1234ze(Z)/isohexane are depicted on Figure 17 and 18, respectively. In all these simulations $PPTD_{ev}$ and $PPTD_{cd}$ was 5 °C, $T_{si,in}$ was 140 °C, $T_{si,out}$ was 200 °C, and $T_{so,in}$ was 120 °C. $T_{so,out}$ varied to make different source temperature glides.

By increasing the source temperature glide, the temperature lift was increased and as result the COP was decreased for both mixtures. For R1234ze(Z)/acetone (Figure 17), the COP obtained by estimated and fitted BIPs are quite similar. However, z_1 changed once the BIPs are fitted. For R1234ze(Z)/isohexane (Figure 18), there is significant difference between COP obtained by estimated and fitted BIPs at different source temperature glides. There is also a significant difference between z_1 obtained by estimated and fitted BIPs.

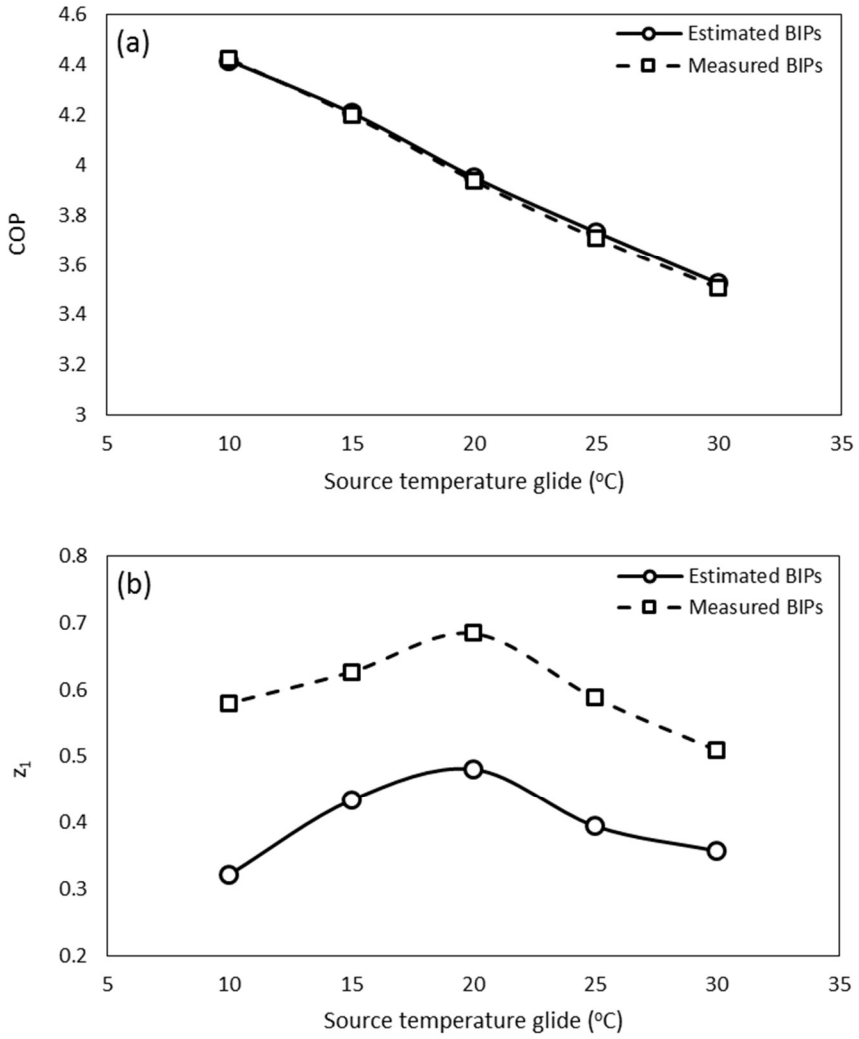

Figure 17. Effect of heat source temperature glide on (a) COP and (b) z_1 for R1234ze(Z)/acetone with estimated and measured (fitted) BIPs.

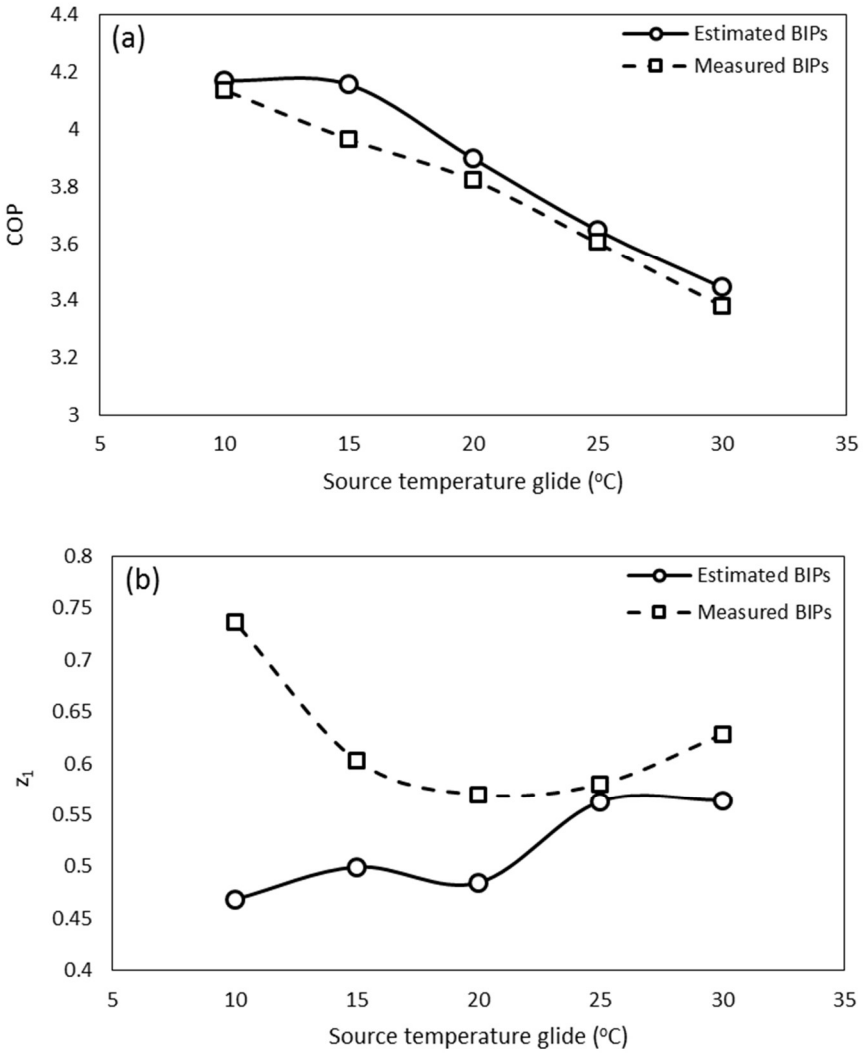

Figure 18. Effect of heat source temperature glide on (a) COP and (b) z_1 for R1234ze(Z)/isohexane with estimated and measured (fitted) BIPs.

4. Conclusions

Zeotropic mixtures are considered as potential working fluids in refrigeration cycles for high temperature heat pumps due to their phase change temperature glide that can be matched with the temperature profile of the sink and the source. In this work, two binary zeotropic mixtures composed of an HFO, R1234ze(Z), and a hydrocarbon, acetone and isohexane, were studied as refrigerants in a HTHP delivering heat up to 200 °C. REFPROP 10.0 was used for thermodynamic calculations. It makes use of binary interaction parameters (BIPs) to estimate physical properties of the mixtures. For several mixtures composed of an HFO, as is the case for the studied mixtures in the present work, BIPs are not available. Therefore, REFPROP 10.0 uses estimated values of BIPs for the calculations. In this study, the BIPs for R1234ze(Z)/acetone and R1234ze(Z)/isohexane were determined experimentally using an isochoric setup. A thermodynamic model combined with an optimization framework was used to simulate the HTHP cycle. The comparison of results using estimated and fitted BIPs shows:

- Both for R1234ze(Z)/acetone and R1234ze(Z)/isohexane the average absolute relative deviations, AARD, between experimental pressures and estimated pressures were reduced drastically once the estimated BIPs were used.
- The range of phase change temperature glide was similar for R1234ze(Z)/acetone with estimated and fitted BIPs. However, the composition corresponding to the maximum temperature glide shifted after tuning the BIPs. For R1234ze(Z)/isohexane, there is a significant difference between the phase change temperature glide using estimated and fitted BIPs. However, the composition corresponding to the maximum temperature glide changed less after tuning the BIPs compared to R1234ze(Z)/acetone.
- HTHP cycle simulation results showed that for R1234ze(Z)/acetone the COP changed slightly by around 0.25% after tuning BIPs. However, the optimum composition of the mixture and cycle parameters (i.e. superheating at the evaporator, evaporator pressure, subcooling at the condenser and condenser pressure) changed significantly after tuning BIPs.
- For the R1234ze(Z)/isohexane, the optimum mixture composition and cycle parameters changed significantly by tuning the BIPs. Moreover, there was around 1.7% difference in the COP obtained by estimated BIPs and fitted BIPs.
- The sensitivity analysis by varying the pinch point temperature difference, sink temperature glide and source temperature glide shows the same trend as those described above for the COP, the mixture composition and the main cycle parameters of the two mixtures by tuning BIPs. .

From the results of this study, it can be concluded that for thermodynamic analysis of zeotropic mixtures, it is important to use fitted BIPs for the specific considered mixture. Relaying on estimated BIPs may lead to different results as it was shown for the two zeotropic mixtures studied in the present work, however the impact is not relevant in the same way for all the performance parameters considered (e.g. COP). Furthermore for high temperature heat pumps application, the selected mixtures represent a valuable option in terms of performance achieved.

5. Acknowledgement

We gratefully acknowledge the financial support of the Flemish Government and Flanders Innovation Entrepreneurship (VLAIO) through the Moonshot project Upheat-INES (HBC.2020.2616).

6. References

1. IEA. Heating without global warming - market developments and policy considerations for renewable heat. 2014.

2. Arpagaus C, Bless F, Uhlmann M, Schiffmann J, Bertsch SS. High temperature heat pumps: Market overview, state of the art, research status, refrigerants, and application potentials. Energy. 2018;152:985-1010.

3. Papapetrou M, Kosmadakis G, Cipollina A, La Commare U, Micale G. Industrial waste heat: Estimation of the technically available resource in the EU per industrial sector, temperature level and country. Applied Thermal Engineering. 2018;138:207-16.

4. Jiang J, Hu B, Wang RZ, Deng N, Cao F, Wang C-C. A review and perspective on industry high-temperature heat pumps. Renewable and Sustainable Energy Reviews. 2022;161:112106.

5. Net Zero by 2050, A Roadmap for the Global Energy Sector, 4th revision, October 2021.

6. Mikielewicz D, Wajs J. Performance of the very high-temperature heat pump with low GWP working fluids. Energy. 2019;182:460-70.

7. Quoilin S, Broek MVD, Declaye S, Dewallef P, Lemort V. Techno-economic survey of Organic Rankine Cycle (ORC) systems. Renewable and Sustainable Energy Reviews. 2013;22:168-86.

8. Dong B, Xu G, Cai Y, Li H. Analysis of zeotropic mixtures used in high-temperature Organic Rankine cycle. Energy Conversion and Management. 2014;84:253-60.

9. Frate GF, Ferrari L, Desideri U. Analysis of suitability ranges of high temperature heat pump working fluids. Applied Thermal Engineering. 2019;150:628-40.

10. Zühlsdorf B, Jensen JK, Cignitti S, Madsen C, Elmegaard B. Analysis of temperature glide matching of heat pumps with zeotropic working fluid mixtures for different temperature glides. Energy. 2018;153:650-60.

11. Abedini H, Vieren E, Demeester T, Beyne W, Lecompte S, Quoilin S, Arteconi A, A Comprehensive Analysis of Binary Mixtures as Working Fluid in Very High Temperature Heat Pumps, Energy Conversion and Managements, 2023, 277, 116652.

12. Lemmon EW, Bell IH, Huber ML, McLinden M.O., NIST Standard Reference Database 23: Reference Fluid Thermodynamic and Transport Properties-REFPROP, Version 10.0, National Institute of Standards and Technology, 2018, URL Http//Www. Nist. Gov/Srd/Nist23. Cfm.

13. World Meteorological Organization, Scientific Assessment of Ozone Depletion: 2018. In: Global Ozone Research and Monitoring Project — Report No. 58, 588 pp., Geneva, Switzerland (2018).

14. https://www.petrochemistry.eu/wp-content/uploads/2018/01/EPD-Phenol-Acetone-10-16.pdf. Accessed: 16-7-2022.

15. Giuliani G, Kumar S, Polonara F. A constant volume apparatus for vapour pressure and gas phase P-v-T measurements: validation with data for R22 and R134a. Fluid Phase Equilibria. 1995;109:265-79.

16. Di Nicola G, Polonara F, Ricci R, Stryjek R. PVTx Measurements for the R116 + CO2 and R41 + CO2 Systems. New Isochoric Apparatus. Journal of Chemical & Engineering Data. 2005;50:312-8.

17. Brown JS, Coccia G, Tomassetti S, Pierantozzi M, Di Nicola G. Vapor Phase PvTx Measurements of Binary Blends of 2,3,3,3-Tetrafluoroprop-1-ene + Isobutane and trans-1,3,3,3-Tetrafluoroprop-1-ene + Isobutane. Journal of Chemical & Engineering Data. 2017;62:3577-84.

18. Brown JS, Coccia G, Tomassetti S, Pierantozzi M, Di Nicola G. Vapor Phase PvTx Measurements of Binary Blends of trans-1-Chloro-3,3,3-trifluoroprop-1-ene + Isobutane and cis-1,3,3,3-Tetrafluoroprop-1-ene + Isobutane. Journal of Chemical & Engineering Data. 2018;63:169-77.

19. Tomassetti S, Coccia G, Pierantozzi M, Di Nicola G, Brown JS. Vapor phase and two-phase PvTz measurements of difluoromethane + 2,3,3,3-tetrafluoroprop-1-ene. The Journal of Chemical Thermodynamics. 2020;141:105966.

20. Bell IH, Riccardi D, Bazyleva A, McLinden MO. Survey of Data and Models for Refrigerant Mixtures Containing Halogenated Olefins. Journal of Chemical & Engineering Data. 2021;66:2335-54.

21. Kunz O, Wagner W. The GERG-2008 Wide-Range Equation of State for Natural Gases and Other Mixtures: An Expansion of GERG-2004. Journal of Chemical & Engineering Data. 2012;57:3032-91.

22. Di Nicola G, Giuliani G, Passerini G, Polonara F, Stryjek R. Vapor–Liquid-Equilibrium (VLE) properties of R-32+R-134a system derived from isochoric measurements. Fluid Phase Equilibria. 1998;153:143-65.

23. Beyer H-G, Schwefel H-P. Evolution strategies – A comprehensive introduction. Natural Computing. 2002;1:3-52.

24. Bell I. H., & Lemmon E. W. Automatic fitting of binary interaction parameters for multi-fluid Helmholtz-energy-explicit mixture models. Journal of Chemical & Engineering Data. 2016;61:3752-3760.

25. Virtanen P, Gommers R, Oliphant TE, Haberland M, Reddy T, Cournapeau D, et al. SciPy 1.0: fundamental algorithms for scientific computing in Python. Nature Methods. 2020;17:261-72.

26. Kosmadakis G, Arpagaus C, Neofytou P, Bertsch S. Techno-economic analysis of high-temperature heat pumps with low-global warming potential refrigerants for upgrading waste heat up to 150 °C. Energy Conversion and Management. 2020;226:113488.

27. Ommen T, Jensen JK, Markussen WB, Reinholdt L, Elmegaard B. Technical and economic working domains of industrial heat pumps: Part 1 – Single stage vapour compression heat pumps. International Journal of Refrigeration. 2015;55:168-82.

7. Appendix

Table A1 and A2 provide the two-phase and the vapor-phase experimental data for R1234ze(Z)/acetone, respectively. The two-phase and the vapor-phase measurements for R1234ze(Z)/isohexane are reported in Table A3 and A4, respectively.

Table A1. Experimentally-determined two-phase values of pressure, p, specific volume, v, temperature, T, and overall experimental mole fraction of R1234ze(Z), z1, for R1234ze(Z)(1)/acetone(2) binary system.[a]

T (°C)	p (bar)	v ($m^3 \cdot kg^{-1}$)	T (°C)	p (bar)	v ($m^3 \cdot kg^{-1}$)
	z_1 = 0.2261			z_1 = 0.4765	
30.00	0.58	0.087952	30.00	0.75	0.171748
35.00	0.69	0.087971	35.00	0.87	0.171786
40.00	0.82	0.087991	40.00	1.00	0.171824
45.00	0.96	0.088010	45.00	1.15	0.171861
50.00	1.13	0.088029	50.00	1.32	0.171899
55.00	1.32	0.088049	55.00 [b]	1.44 [b]	0.171937 [b]
60.00	1.53	0.088068	60.00 [b]	1.54 [b]	0.171974 [b]
65.00	1.77	0.088087			
70.00	2.03	0.088107			
75.00	2.33	0.088126			

T (°C)	p (bar)	v ($m^3 \cdot kg^{-1}$)	T (°C)	p (bar)	v ($m^3 \cdot kg^{-1}$)
80.00	2.65	0.088145			
85.00	3.03	0.088164			
90.00	3.42	0.088184			
95.00[b]	3.83[b]	0.088203[b]			
	z_1 = 0.3831			z_1 = 0.5137	
30.00	0.67	0.177411	30.00	0.86	0.128783
35.00	0.78	0.177450	35.00	0.98	0.128811
40.00	0.91	0.177489	40.00	1.13	0.128839
45.00	1.06	0.177528	45.00	1.30	0.128867
50.00	1.21	0.177567	50.00	1.48	0.128896
55.00	1.38	0.177606	55.00	1.68	0.128924
60.00[b]	1.51[b]	0.177645[b]	60.00	1.88	0.128952
65.00[b]	1.63[b]	0.177684[b]	65.00[b]	2.00[b]	0.128980[b]
	z_1 = 0.4081			z_1 = 0.6653	
30.00	0.78	0.083127	30.00	1.06	0.123881
35.00	0.92	0.083146	35.00	1.21	0.123908
40.00	1.07	0.083164	40.00	1.37	0.123935
45.00	1.24	0.083182	45.00	1.55	0.123962
50.00	1.43	0.083200	50.00	1.74	0.123990
55.00	1.65	0.083219	55.00[b]	1.89[b]	0.124017[b]
60.00	1.89	0.083237			
65.00	2.15	0.083255			
70.00	2.44	0.083273			
75.00	2.76	0.083292			
80.00	3.08	0.083310			
85.00[b]	3.42[b]	0.083328[b]			

[a]Expanded uncertainties are $U(T)$ = 0.03 °C, $U(p)$ = 0.01 bar, $U(v)$ = 0.337 $dm^3 \cdot kg^{-1}$ and $U(z_1)$ = 0.003.
[b]Not considered in the calculations.

Table A2. Experimentally-determined vapor-phase values of pressure, p, specific volume, v, temperature, T, and overall experimental mole fraction of R1234ze(Z), z_1, for R1234ze(Z)(1)/acetone(2) binary system.[a]

T (°C)	p (bar)	v ($m^3 \cdot kg^{-1}$)	T (°C)	p (bar)	v ($m^3 \cdot kg^{-1}$)
	z_1 = 0.2261			z_1 = 0.4765	
100.00[b]	4.14[b]	0.088222[b]	65.00[b]	1.64[b]	0.172012[b]
105.00[b]	4.34[b]	0.088242[b]	70.00[b]	1.73[b]	0.172050[b]
110.00	4.46	0.088261	75.00	1.82	0.172087
115.00	4.56	0.088280	80.00	1.86	0.172125
			85.00	1.90	0.172163
			90.00	1.93	0.172200
			95.00	1.97	0.172238
			100.00	2.00	0.172276

T (°C)	p (bar)	v ($m^3 \cdot kg^{-1}$)	T (°C)	p (bar)	v ($m^3 \cdot kg^{-1}$)
			105.00	2.03	0.172313
			110.00	2.07	0.172351
	z_1 = 0.3831			z_1 = 0.5137	
70.00 [b]	1.74 [b]	0.177723 [b]	70.00 [b]	2.13 [b]	0.129009 [b]
75.00 [b]	1.88 [b]	0.177762 [b]	75.00 [b]	2.24 [b]	0.129037 [b]
80.00	1.92	0.177801	80.00 [b]	2.35 [b]	0.129065 [b]
85.00	1.96	0.177840	85.00	2.42	0.129093
90.00	2.00	0.177879	90.00	2.47	0.129122
95.00	2.03	0.177917	95.00	2.53	0.129150
100.00	2.06	0.177956	100.00	2.58	0.129178
105.00	2.10	0.177995	105.00	2.62	0.129206
110.00	2.13	0.178034	110.00	2.66	0.129235
	z_1 = 0.4081			z_1 = 0.6653	
90.00 [b]	3.61 [b]	0.083346 [b]	60.00 [b]	1.99 [b]	0.124044 [b]
95.00 [b]	3.83 [b]	0.083365 [b]	65.00 [b]	2.06 [b]	0.124071 [b]
100.00	4.03	0.083383	70.00	2.20	0.124098
105.00	4.13	0.083401	75.00	2.25	0.124125
110.00	4.21	0.083419	80.00	2.30	0.124153
115.00	4.29	0.083437	85.00	2.34	0.124180
			90.00	2.39	0.124207
			95.00	2.44	0.124234
			100.00	2.48	0.124261
			105.00	2.52	0.124289

[a]Expanded uncertainties are $U(T)$ = 0.03 °C, $U(p)$ = 0.01 bar, $U(v)$ = 0.337 $dm^3 \cdot kg^{-1}$ and $U(z_1)$ = 0.003.
[b]Not considered in the calculations.

Table A3. Experimentally-determined two-phase values of pressure, p, specific volume, v, temperature, T, and overall experimental mole fraction of R1234ze(Z), z_1, for R1234ze(Z)(1)/isohexane(2) binary system.[a]

T (°C)	p (bar)	v ($m^3 \cdot kg^{-1}$)	T (°C)	p (bar)	v ($m^3 \cdot kg^{-1}$)
	z_1 = 0.2568			z_1 = 0.5614	
40.00	1.32	0.065544	25.00	1.17	0.128327
45.00	1.46	0.065559	30.00	1.27	0.128355
50.00	1.60	0.065573	35.00	1.37	0.128384
55.00	1.77	0.065587	40.00	1.49	0.128412
60.00	1.95	0.065602	45.00	1.62	0.128440
65.00	2.14	0.065616	50.00	1.75	0.128468
70.00	2.36	0.065630	55.00[b]	1.88[b]	0.128496[b]
75.00	2.60	0.065645			
80.00	2.87	0.065659			
85.00	3.16	0.065674			
90.00	3.48	0.065688			
95.00	3.82	0.065702			
100.00[b]	4.16[b]	0.065717[b]			
	z_1 = 0.4615			z_1 = 0.5977	
25.00	0.87	0.175690	20.00	1.03	0.147377
30.00	0.94	0.175729	25.00	1.12	0.147409
35.00	1.03	0.175768	30.00	1.22	0.147442
40.00	1.13	0.175806	35.00	1.32	0.147474
45.00	1.25	0.175845	40.00	1.42	0.147506
50.00	1.36	0.175883	45.00	1.55	0.147539
	z_1 = 0.5050			z_1 = 0.7559	
30.00	1.55	0.074686	25.00	1.66	0.067806
35.00	1.70	0.074702	30.00	1.93	0.067821
40.00	1.87	0.074719	35.00	2.22	0.067836
45.00	2.03	0.074735	40.00	2.50	0.067851
50.00	2.21	0.074752	45.00[b]	2.78[b]	0.067866[b]
55.00	2.39	0.074768	50.00[b]	3.02[b]	0.067881[b]
60.00	2.59	0.074784			
65.00	2.80	0.074801			
70.00	3.03	0.074817			
75.00[b]	3.26[b]	0.074833[b]			

[a]Expanded uncertainties are $U(T)$ = 0.03 °C, $U(p)$ = 0.01 bar, $U(v)$ = 0.332 $dm^3 \cdot kg^{-1}$ and $U(z_1)$ = 0.002.
[b]Not considered in the calculations.

Table A4. Experimentally-determined vapor-phase values of pressure, *p*, specific volume, *v*, temperature, *T*, and overall experimental mole fraction of R1234ze(Z), z_1, for R1234ze(Z)(1)/isohexane(2) binary system.[a]

T (°C)	*p* (bar)	*v* ($m^3 \cdot kg^{-1}$)	*T* (°C)	*p* (bar)	*v* ($m^3 \cdot kg^{-1}$)
	z_1 = 0.2568			z_1 = 0.5614	
105.00[b]	4.42[b]	0.065731[b]	60.00[b]	1.95[b]	0.128524[b]
107.50[b]	4.49[b]	0.065738[b]	65.00[b]	1.99[b]	0.128553[b]
110.00	4.55	0.065745	70.00	2.03	0.128581
112.50	4.60	0.065753	75.00	2.06	0.128609
115.00	4.64	0.065760	80.00	2.10	0.128637
117.50	4.67	0.065767	85.00	2.14	0.128665
			90.00	2.17	0.128693
			95.00	2.20	0.128721
			100.00	2.24	0.128750
			105.00	2.27	0.128778
			110.00	2.31	0.128806
	z_1 = 0.4615			z_1 = 0.5977	
55.00[b]	1.44[b]	0.175922[b]	50.00[b]	1.63[b]	0.147571[b]
60.00[b]	1.48[b]	0.175960[b]	55.00[b]	1.67[b]	0.147603[b]
65.00	1.52	0.175999	60.00	1.71	0.147636
70.00	1.55	0.176037	65.00	1.74	0.147668
75.00	1.58	0.176076	70.00	1.77	0.147701
80.00	1.60	0.176115	75.00	1.80	0.147733
85.00	1.63	0.176153	80.00	1.83	0.147765
90.00	1.66	0.176192	85.00	1.86	0.147798
95.00	1.68	0.176230	90.00	1.89	0.147830
100.00	1.71	0.176269	95.00	1.93	0.147862
105.00	1.73	0.176307	100.00	1.95	0.147895
110.00	1.76	0.176346	105.00	1.98	0.147927
			110.00	2.01	0.147959
	z_1 = 0.5050			z_1 = 0.7559	
80.00[b]	3.44[b]	0.074850[b]	55.00[b]	3.22[b]	0.067895[b]
85.00[b]	3.54[b]	0.074866[b]	60.00[b]	3.36[b]	0.067910[b]
90.00	3.62	0.074883	65.00	3.44	0.067925
95.00	3.69	0.074899	70.00	3.52	0.067940
100.00	3.75	0.074915	75.00	3.58	0.067955
105.00	3.82	0.074932	80.00	3.65	0.067970
110.00	3.88	0.074948	85.00	3.71	0.067985
115.00	3.94	0.074965	90.00	3.78	0.068000
			95.00	3.84	0.068015
			100.00	3.90	0.068029
			105.00	3.97	0.068044
			110.00	4.03	0.068059

[a]Expanded uncertainties are $U(T)$ = 0.03 °C, $U(p)$ = 0.01 bar, $U(v)$ = 0.332 $dm^3 \cdot kg^{-1}$ and $U(z_1)$ = 0.002.
[b]Not considered in the calculations.